2.8. Statistical analysis

Comparisons between experimental groups were performed by two-tailed Student's *t*-test. Values of $p < 0.05$ were considered significant unless otherwise indicated.

3. Results

3.1. Protective effect of intranasal immunisation with CTB*-combined vaccine against H5N1 (HK483) infection in BALB/c and B10 mice

Influenza virus H5N1 HA-specific IgA and IgG responses and protection against virus infection were examined in BALB/c and B10 mice immunised intranasally with two doses of HA-modified recombinant virus (H5N1) vaccine combined with CTB* (Fig. 1). BALB/c mice are high responders to the HA molecule of H1N1 influenza virus, while B10 mice are low responders. The immunisation protocol was as described in Section 2. All groups of BALB/c or B10 mice immunised with vaccine with CTB* showed HA-reactive mucosal IgA and IgG responses and serum IgG responses (Fig. 1). Vaccinated mice were also resistant against lethal challenge by H5N1 virus, while non-immunized mice were sensitive to the virus challenge (Fig. 1). Thus, intranasal administration of vaccine with CTB* was effective against H5N1 virus infection in both BALB/c and B10 mice.

3.2. Comparison of antibody responses and protective effects against H5N1 (HK483) infection in mice vaccinated with adjuvants, CTB*, poly (I:C), CMP, and poly (I:C) + CMP

To compare the adjuvant effects of poly (I:C) and CMP with CTB*, the antibody responses to H5-HA molecules were examined in BALB/c mice immunised intranasally with the vaccine and these adjuvants. The immunisation and experimental protocol was performed as described in the Materials and Methods. As we reported the effective doses of CTB*, poly (I:C) and CMP previously [20,21], we used 1 μg of CTB*, 10 μg of poly (I:C), and 10 μg or 100 μg of CMP for vaccination.

Among the adjuvants used, including CTB*, poly (I:C), CMP and poly (I:C) + CMP, CTB* induced the highest nasal IgA and serum IgG antibody titres to H5-HA, while poly (I:C) + CMP elicited weaker IgA antibody responses in the nasal wash (Fig. 2). The levels of production of IgA against H5-HA in the nasal wash in mice administered either poly (I:C) or CMP were relatively low (Fig. 2). Intranasal vaccination without adjuvant failed to induce antibody responses (Fig. 2). Subcutaneous immunisation with H5N1 vaccine without adjuvant also failed to induce antibody responses (data not shown). Thus, the use of an appropriate adjuvant enhances the efficiency of antibody production in H5N1 vaccination.

Next, we compared the protective effects of intranasal administration of the vaccine in combination with various adjuvants against lethal H5N1 infection. The time courses of survival rate and body weight loss of mice infected with H5N1 were examined for 18 days (Fig. 3A,B). After challenge infection with H5N1 (HK483) virus, non-immunised mice showed a loss of body weight with deterioration of clinical signs, such as ruffled fur, inactivity and paralysis of posterior limb. In the non-immunised group, none of the mice survived for more than 12 days after challenge infection. In contrast, none of the mice died in the groups vaccinated intranasally along with either 1 μg of CTB* or 10 μg each of poly (I:C) + CMP without any clinical signs for 18 days (Fig. 3A). Some mice in the groups vaccinated along with either poly (I:C) or CMP showed clinical signs, including a slight decrease in body weight (Fig. 3B), and died at 8 days after infection (Fig. 3A). These observations suggested that intranasal vaccination with either CTB* or concurrent use of poly (I:C) and CMP as adjuvants provided complete protection against lethal H5N1 influenza virus challenge for at least 18 days, and these protective effects seemed to be correlated with the levels of antibody production in the nasal wash and serum.

3.3. Antibody-forming cells (AFC) in the NALT and spleen of mice vaccinated intranasally with adjuvants

To examine the mechanism of intranasal vaccination, the responses of IgA AFC, IgG AFC and IgM AFC in the NALT and spleen against modified-H5-HA protein were examined in mice 2 weeks after second intranasal immunisation of vaccine with various adjuvants (Fig. 4). The numbers of IgA AFC and IgG AFC in the NALT were higher in the groups vaccinated with CTB* and poly (I:C) + CMP than in the other groups (Fig. 4). The group vaccinated with CTB* showed greater numbers of AFC cells than the other groups (Fig. 4). The number of IgM AFC in the spleen was greater in the group vaccinated with poly (I:C) + CMP than in the other groups. These results suggested that poly (I:C) + CMP as an adjuvant showed a synergistic effect on induction of AFC in the NALT as well as CTB*.

3.4. Pathological findings of the H5N1 (HK483) infected mice vaccinated intranasally with poly (I:C) + CMP

We next examined the pathological findings in non-immunised mice in comparison with those immunised intranasally with H5N1 vaccine and poly (I:C) + CMP after fatal virus challenge. Large amounts of mucous material and necrosis of the columnar epithelial cells were observed in the nasal

Fig. 5. Histopathological findings of the nasal cavity (A–D) (×40) and brain (E–H) (×100) of mice immunised intranasally with H5 vaccine with poly (I:C) + CMP (C, D, G and H) or non-immunised controls (A, B, E and F) followed by 100 LD_{50} HK483 virus infection. (×40, H&E (A, C, E, G) or ×40, anti-nucleoprotein (NP) immunostaining (B, D, F and H)). Specimens were collected 8 days after virus challenge. The insets in Fig. 5B,F are higher magnification (×200) of Fig. 5B,F. The scale bar shows 500 μm (A–D) or 200 μm (E–H).

cavity in non-immunised mice (Fig. 5A), and viral antigen was detected in the mucous material (Fig. 5B). Marked inflammatory cell infiltration with widely distributed viral antigen was also observed in the cerebrum and brainstem of non-immunised mice, consistent with viral encephalitis (Fig. 5E,F). In higher magnification, neurons are predominantly stained with anti-NP antibody (inset of Fig. 5F). Viral antigen-positive cells were much more frequent in the central nervous system than in the nasal cavity. No pathological changes and no viral antigen were detected in other organs, including the lungs and heart (data not shown). No pathological changes (Fig. 5C,G) or viral antigens (Fig. 5D,H) were detected in the nasal cavity, cerebrum or brainstem of immunised mice.

3.5. Expression of mRNAs of Toll-like receptors in the NALT and spleen of mice vaccinated intranasally with adjuvants

To determine the mechanism of action of influenza HA vaccine administered intranasally with adjuvants, we initially examined mRNA expression levels of Toll-like receptors (TLRs), including TLR3, TLR4 and TLR7, which are receptors of double-stranded RNA, lipopolysaccharide and single-stranded RNA, respectively. The levels of expression of both TLR3 and TLR7 mRNAs in the NALT of mice vaccinated with either poly (I:C) or poly (I:C) + CMP were significantly greater than those of mice vaccinated without adjuvants (7.8–12.7-fold; $p < 0.05$, Fig. 6A). TLR4 expression was significantly increased exclusively in mice vaccinated with CTB* ($p < 0.05$). These results suggested that up-regulation of TLR3 in the NALT may enhance the adjuvant effect of poly (I:C), which is consistent with a previous report [20]. In the spleen, the levels of TLR3, TLR4 and TLR7 mRNAs were slightly higher in the poly (I:C) + CMP group than the other groups (Fig. 6B). These observations suggested that the expression of TLR3 and TLR7 mRNAs in the NALT and spleen may affect expression of cytokines and production of antibodies.

4. Discussion

Until recently, direct transmission of avian influenza viruses to the human respiratory system has been considered very rare. However, it has been reported that some subtypes of avian influenza virus can replicate in the human respiratory tract after experimental infection [28]. In addition, at least 56 people died in Vietnam and Thailand between late 2003 and late 2005 (WHO), which is known as the "East Asian H5N1 epizoonotic period" [29]. The development of an effective vaccine offer the best strategy to protect humans against the

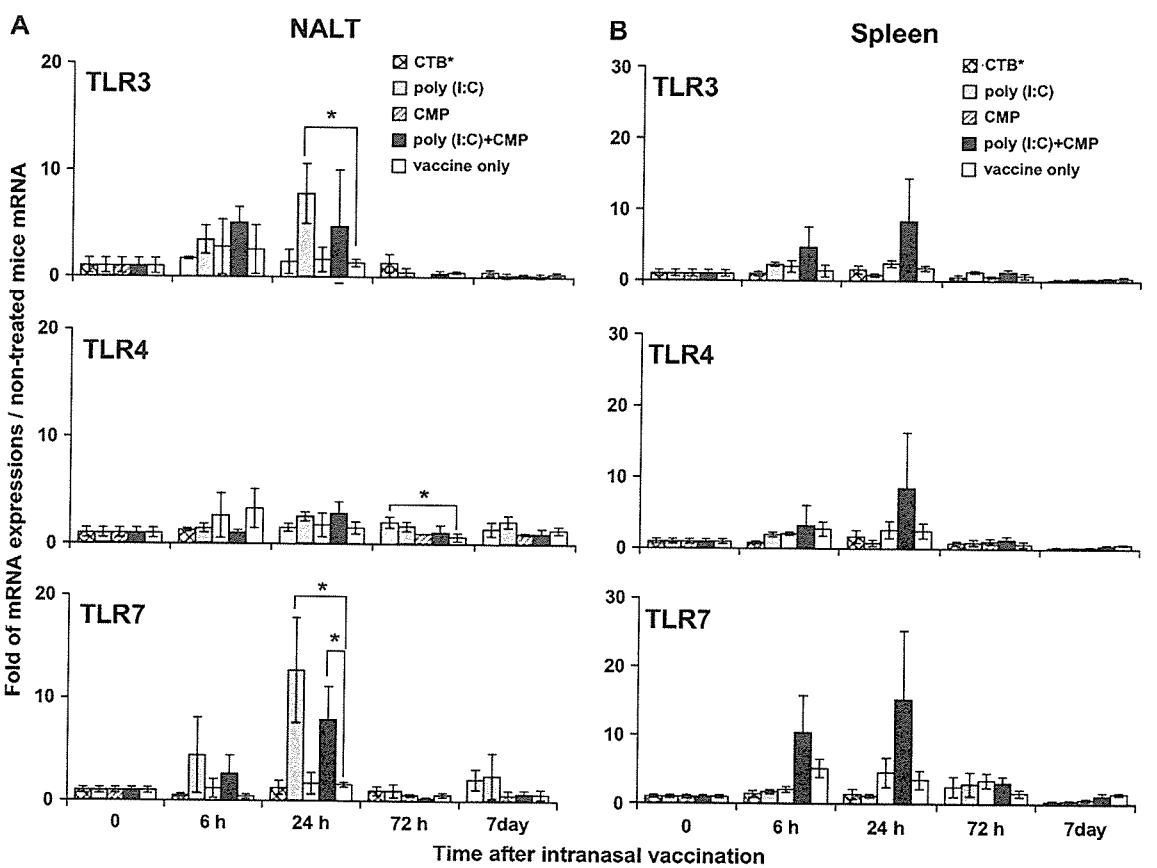

Fig. 6. Expression of TLR3, TLR4 and TLR7 mRNAs in the NALT and spleen of mice immunised intranasally with H5 vaccine with CTB*, poly (I:C), CMP or poly (I:C) + CMP at various time points (0, 6, 24, 72 h and 7 days) after vaccination. To determine the expression levels of TLR3, TLR4 or TLR7 mRNA in the NALT (A) or spleen (B), real-time quantitative RT-PCR assays were performed ($n = 3$). Comparisons between the two groups were performed with the t-test for paired observations. *$p < 0.05$.

emergence of avian influenza virus that has developed high transmissibility to humans.

As the multibasic sequence cleavage site contributes to the pathogenesis of human H5N1 infection, attenuation of the virus with modified haemagglutinin for vaccine production has been established by a plasmid-based reverse genetics system [5]. We have also prepared avirulent recombinant H5N1 (HK9-1-1) virus by reverse genetics by removal of the multibasic amino acid motif at the haemagglutinin cleavage site [23].

In 1999, Takada et al. reported that formalin-inactivated HK9-1-1 vaccine induced protective immunity in mice intranasally administered high doses (100 μg × 3 times) of vaccine [23]. As it is assumed that the supply of vaccine against the virus would be limited should the emerging virus become a pandemic, an adjuvant capable of enhancing the immunogenicity of the vaccine would conserve stocks. It has been reported that intranasal administration of inactivated vaccine with appropriate adjuvant induces higher titres of antigen-specific mucosal IgA and systemic IgG than the subcutaneous route. In addition, intranasal vaccination induces cross-reactive S-IgA antibodies that can recognize variant viruses and effectively block influenza virus infection at the mucosal membrane, which is the initial target site [11,20,21].

Bacterial toxin-derived adjuvants, such as CT and CTB have been proposed as adjuvants for mucosal vaccination [30]. Although CT is classified as a Th2-type adjuvant, it provokes nasal discharge and paralysis of facial nerves. As the nasal cavity and the forebrain have direct communication *via* the olfactory nerve, the safety of nasal administration of vaccination with adjuvant for the central nervous system needs to be considered. The safety of poly (I:C) for the central nervous system has already been confirmed by direct intracerebral injection of poly (I:C) [20]. Previously, we reported that both CMP [21] and poly (I:C) [20] are effective against H1N1 influenza vaccine by intranasal administration. However, the results of the present study demonstrated that concomitant administration of poly (I:C) + CMP was more effective than either poly (I:C) or CMP alone. In addition, poly(I:C) + CMP or poly(I:C) adjuvant is more efficient than CMP alone. Intranasal vaccination with poly (I:C) + CMP strongly enhanced nasal IgA and serum IgG against H5 HA (Fig. 2), and induced IgA- and IgG-producing AFCs in the NALT to a greater extent than vaccination with CTB* (Fig. 3). The mechanisms of the adjuvant effect of dsRNA and CMP are still unclear; however, it is known that after recognition by TLR3, RNA helicase, and retinoic acid-inducible gene I, dsRNA can activate the NF-κB pathway and production of IFN [17,31]. Early administration of IFN-α/β during an immune response markedly increases primary antibody response against soluble antigens [18]. Intranasal application of small doses (10–100 μg) of CMP has been shown to result in an elevation of Th1 cytokines, such as IL-12, IFN-γ, and TNF-α, and reduction of IL-4 production during allergen challenge [22]. It is suggested that these synergistic effects of both poly (I:C) and CMP result in marked antibody responses together with enhancement of expression of mRNAs of TLR3, TLR4, TLR7, IFN-γ, and IL-6, and confer complete protection against lethal challenge with H5N1. The use of poly (I:C) and CMP in combination enhances the cytokine responses in the spleen more effectively than the single use of poly (I:C) or CMP, and results in the enhancement of the systemic immune response. CMP can act as a carrier for poly (I:C). In addition, IFN-γ expression was enhanced in the spleen following administration of both poly (I:C) and CMP. The synergistic effects may contribute to the enhancement of mucosal adjuvant effects leading to complete protection against viral challenge.

Acknowledgements

We are grateful to Ms. Y. Sato and Ms. A. Harashima for excellent technical assistance, and Dr. W.W. Hall for helpful discussion. This work was supported by grants for Research on Health Sciences focusing on Drug Innovation and from the Ministry of Health, Labour and Welfare.

Reference

[1] E.C. Claas, A.D. Osterhaus, R. van Beek, J.C. De Jong, G.F. Rimmelzwaan, D.A. Senne, S. Krauss, K.F. Shortridge, R.G. Webster, Human influenza A H5N1 virus related to a highly pathogenic avian influenza virus, Lancet 351 (1998) 472–477.

[2] J.C. de Jong, E.C. Claas, A.D. Osterhaus, R.G. Webster, W.L. Lim, A pandemic warning? Nature 389 (1997) 554.

[3] J.S. Peiris, W.C. Yu, C.W. Leung, C.Y. Cheung, W.F. Ng, J.M. Nicholls, T.K. Ng, K.H. Chan, S.T. Lai, W.L. Lim, K.Y. Yuen, Y. Guan, Re-emergence of fatal human influenza A subtype H5N1 disease, Lancet 363 (2004) 617–619.

[4] K.F. Shortridge, N.N. Zhou, Y. Guan, P. Gao, T. Ito, Y. Kawaoka, S. Kodihalli, S. Krauss, D. Markwell, K.G. Murti, M. Norwood, D. Senne, L. Sims, A. Takada, R.G. Webster, Characterization of avian H5N1 influenza viruses from poultry in Hong Kong, Virology 252 (1998) 331–342.

[5] K. Subbarao, H. Chen, D. Swayne, L. Mingay, E. Fodor, G. Brownlee, X. Xu, X. Lu, J. Katz, N. Cox, Y. Matsuoka, Evaluation of a genetically modified reassortant H5N1 influenza A virus vaccine candidate generated by plasmid-based reverse genetics, Virology 305 (2003) 192–200.

[6] F.M. Davenport, A.V. Hennessy, F.M. Brandon, R.G. Webster, C.D. Barrett Jr., G.O. Lease, Comparisons of serologic and febrile responses in humans to vaccination with influenza a viruses or their hemagglutinins, J. Lab. Clin. Med 63 (1964) 5–13.

[7] R.B. Couch, J.A. Kasel, Immunity to influenza in man, Annu. Rev. Microbiol. 37 (1983) 529–549.

[8] B.R. Murphy, Mucosal immunity to viruses, in: P.L. Ogra, M.E. Lamm, J.R. McGhee, J. Mestecky, W. Strober, J. Bienenstock (Eds.), Handbook of Mucosal Immunology, Academic Press, 1994, p. 333.

[9] K.B. Renegar, P.A. Small Jr., L.G. Boykins, P.F. Wright, Role of IgA versus IgG in the control of influenza viral infection in the murine respiratory tract, J. Immunol 173 (2004) 1978–1986.

[10] S. Tamura, Y. Ito, H. Asanuma, Y. Hirabayashi, Y. Suzuki, T. Nagamine, C. Aizawa, T. Kurata, Cross-protection against influenza virus infection afforded by trivalent inactivated vaccines inoculated intranasally with cholera toxin B subunit, J. Immunol 149 (1992) 981–988.

[11] Y. Asahi, T. Yoshikawa, I. Watanabe, T. Iwasaki, H. Hasegawa, Y. Sato, S. Shimada, M. Nanno, Y. Matsuoka, M. Ohwaki, Y. Iwakura, Y. Suzuki, C. Aizawa, T. Sata, T. Kurata, S. Tamura, Protection against influenza virus infection in polymeric Ig receptor knockout mice immunized intranasally with adjuvant-combined vaccines, J. Immunol 168 (2002) 2930–2938.

[12] Y. Asahi-Ozaki, T. Yoshikawa, Y. Iwakura, Y. Suzuki, S. Tamura, T. Kurata, T. Sata, Secretory IgA antibodies provide cross-protection

against infection with different strains of influenza B virus, J. Med. Virol 74 (2004) 328–335.
[13] R.B. Couch, Nasal vaccination, *Escherichia coli* enterotoxin, and Bell's palsy, N. Engl. J. Med 350 (2004) 860–861.
[14] Y. Hagiwara, K. Komase, Z. Chen, K. Matsuo, Y. Suzuki, C. Aizawa, T. Kurata, S. Tamura, Mutants of cholera toxin as an effective and safe adjuvant for nasal influenza vaccine, Vaccine 17 (1999) 2918–2926.
[15] I. Watanabe, T.M. Ross, S. Tamura, T. Ichinohe, S. Ito, H. Takahashi, H. Sawa, J. Chiba, T. Kurata, T. Sata, H. Hasegawa, Protection against influenza virus infection by intranasal administration of C3d-fused hemagglutinin, Vaccine 21 (2003) 4532–4538.
[16] B.L. Jacobs, J.O. Langland, When two strands are better than one: the mediators and modulators of the cellular responses to double-stranded RNA, Virology 219 (1996) 339–349.
[17] L. Alexopoulou, A.C. Holt, R. Medzhitov, R.A. Flavell, Recognition of double-stranded RNA and activation of NF-kappaB by Toll-like receptor 3, Nature 413 (2001) 732–738.
[18] A. Le Bon, G. Schiavoni, G. D'Agostino, I. Gresser, F. Belardelli, D.F. Tough, Type i interferons potently enhance humoral immunity and can promote isotype switching by stimulating dendritic cells in vivo, Immunity 14 (2001) 461–470.
[19] S.S. Diebold, T. Kaisho, H. Hemmi, S. Akira, C. Reis e Sousa, Innate antiviral responses by means of TLR7-mediated recognition of single-stranded RNA, Science 303 (2004) 1529–1531.
[20] T. Ichinohe, I. Watanabe, S. Ito, H. Fujii, M. Moriyama, S. Tamura, H. Takahashi, H. Sawa, J. Chiba, T. Kurata, T. Sata, H. Hasegawa, Synthetic double-stranded RNA poly(I:C) combined with mucosal vaccine protects against influenza virus infection, J. Virol 79 (2005) 2910–2919.
[21] H. Hasegawa, T. Ichinohe, P. Strong, I. Watanabe, S. Ito, S. Tamura, H. Takahashi, H. Sawa, J. Chiba, T. Kurata, T. Sata, Protection against influenza virus infection by intranasal administration of hemagglutinin vaccine with chitin microparticles as an adjuvant, J. Med. Virol 75 (2005) 130–136.
[22] P. Strong, H. Clark, K. Reid, Intranasal application of chitin microparticles down-regulates symptoms of allergic hypersensitivity to *Dermatophagoides pteronyssinus* and *Aspergillus fumigatus* in murine models of allergy, Clin. Exp. Allergy 32 (2002) 1794–1800.
[23] A. Takada, N. Kuboki, K. Okazaki, A. Ninomiya, H. Tanaka, H. Ozaki, S. Itamura, H. Nishimura, M. Enami, M. Tashiro, K.F. Shortridge, H. Kida, Avirulent Avian influenza virus as a vaccine strain against a potential human pandemic, J. Virol 73 (1999) 8303–8307.
[24] R.A. Yetter, S. Lehrer, R. Ramphal, P.A. Small Jr., Outcome of influenza infection: effect of site of initial infection and heterotypic immunity, Infect. Immun 29 (1980) 654–662.
[25] H. Asanuma, A.H. Thompson, T. Iwasaki, Y. Sato, Y. Inaba, C. Aizawa, T. Kurata, S. Tamura, Isolation and characterization of mouse nasal-associated lymphoid tissue, J. Immunol. Methods 202 (1997) 123–131.
[26] C.C. Czerkinsky, L.A. Nilsson, H. Nygren, O. Ouchterlony, A. Tarkowski, A solid-phase enzyme-linked immunospot (ELISPOT) assay for enumeration of specific antibody-secreting cells, J. Immunol. Methods 65 (1983) 109–121.
[27] H. Nishimura, S. Itamura, T. Iwasaki, T. Kurata, M. Tashiro, Characterization of human influenza A (H5N1) virus infection in mice: neuro-, pneumo- and adipotropic infection, J. Gen. Virol 81 (2000) 2503–2510.
[28] M.N. Matrosovich, T.Y. Matrosovich, T. Gray, N.A. Roberts, H.D. Klenk, Human and avian influenza viruses target different cell types in cultures of human airway epithelium, Proc. Natl. Acad. Sci. USA 101 (2004) 4620–4624.
[29] T.T. Hien, M. de Jong, J. Farrar, Avian influenza – a challenge to global health care structures, N. Engl. J. Med 351 (2004) 2363–2365.
[30] S. Tamura, A. Yamanaka, M. Shimohara, T. Tomita, K. Komase, Y. Tsuda, Y. Suzuki, T. Nagamine, K. Kawahara, H. Danbara, Synergistic action of cholera toxin B subunit (and *Escherichia coli* heat-labile toxin B subunit) and a trace amount of cholera whole toxin as an adjuvant for nasal influenza vaccine, Vaccine 12 (1994) 419–426.
[31] M. Yoneyama, M. Kikuchi, T. Natsukawa, N. Shinobu, T. Imaizumi, M. Miyagishi, K. Taira, S. Akira, T. Fujita, The RNA helicase RIG-I has an essential function in double-stranded RNA-induced innate antiviral responses, Nat. Immunol 5 (2004) 730–737.

CLINICAL AND DIAGNOSTIC LABORATORY IMMUNOLOGY, July 2005, p. 848–854 Vol. 12, No. 7
1071-412X/05/$08.00+0 doi:10.1128/CDLI.12.7.848–854.2005

Evaluation of Inapparent Nosocomial Severe Acute Respiratory Syndrome Coronavirus Infection in Vietnam by Use of Highly Specific Recombinant Truncated Nucleocapsid Protein-Based Enzyme-Linked Immunosorbent Assay

Fuxun Yu,[1] Mai Quynh Le,[2] Shingo Inoue,[1] Hong Thi Cam Thai,[1] Futoshi Hasebe,[1] Maria del Carmen Parquet,[1] and Kouichi Morita[1]*

Department of Virology, Institute of Tropical Medicine, Nagasaki University, 1-12-4 Sakamoto, Nagasaki 852-8523, Japan,[1] and Department of Virology, National Institute of Hygiene and Epidemiology (NIHE), Hanoi, Vietnam[2]

Received 24 January 2005/Returned for modification 6 April 2005/Accepted 18 April 2005

Severe acute respiratory syndrome (SARS) is a recently emerged human disease associated with pneumonia. Inapparent infection with SARS coronavirus (CoV) is not well characterized. To develop a safe, simple, and reliable screening method for SARS diagnosis and epidemiological study, two recombinant SARS-CoV nucleocapsid proteins (N′ protein and $N\Delta_{121}$ protein) were expressed in *Escherichia coli*, purified by affinity chromatography, and used as antigens for indirect, immunoglobulin G enzyme-linked immunosorbent assays (ELISA). Serum samples collected from healthy volunteers and SARS patients in Vietnam were used to evaluate the newly developed methods. The N′ protein-based ELISA showed a highly nonspecific reaction. The $N\Delta_{121}$ protein-based ELISA, with a nonspecific reaction drastically reduced compared to that of the nearly-whole-length N′ protein-based ELISA, resulted in higher rates of positive reactions, higher titers, and earlier detection than the SARS-CoV-infected cell lysate-based ELISA. These results indicate that our newly developed SARS-CoV $N\Delta_{121}$ protein-based ELISA is not only safe but also a more specific and more sensitive method to diagnose SARS-CoV infection and hence a useful tool for large-scale epidemiological studies. To identify inapparent SARS-CoV infections, serum samples collected from health care workers (HCWs) in Vietnam were screened by the $N\Delta_{121}$ protein-based ELISA, and positive samples were confirmed by a virus neutralization test. Four out of 149 HCWs were identified to have inapparent SARS-CoV infection in Vietnam, indicating that subclinical SARS-CoV infection in Vietnam is rare but does exist.

Severe acute respiratory syndrome (SARS) is a recently emerged human disease associated with pneumonia. The first outbreak was recognized in late February 2003 in Hanoi, Vietnam, and was believed to have originated in November 2002 in the Guangdong province of China with several hundred cases of severe atypical pneumonia (2, 8, 18, 26). Following the detection of similar cases in Hong Kong and Canada, the World Health Organization (WHO) issued a global alert for the illness and later designated it SARS (12, 17, 22). The disease has since affected 30 countries on five continents, with more than 8,400 cases and more than 900 deaths. The identification of the virus and subsequent unraveling of the SARS coronavirus (CoV) genome sequence are important from a public health perspective. The SARS-CoV genome is about 29 kb in size and comprises 11 open reading frames. It contains a well-conserved region encoding an RNA-dependent RNA polymerase with two open reading frames, a variable region encoding four viral structural proteins (spike [S] protein, envelope [E] protein, membrane [M] protein, and nucleocapsid [N] protein), and five putative genes encoding uncharacterized proteins (15, 18). Its gene order is similar to that of the other known coronaviruses; however, phylogenetic analyses and sequence comparisons indicate that this virus does not closely resemble any of the previously characterized coronaviruses.

The epidemiology of SARS remains poorly understood. It is still unclear whether SARS-CoV asymptomatic infection exists. Such information is important not only to understand the virulence of the virus and its pathogenesis but also to identify potential implications for the transmission and control of SARS. The existing reports about nonpneumonic and subclinical SARS coronavirus infections are conflicting. On one hand, Chan et al. and Chow et al. reported that no subclinical infection was found among health care workers (HCWs) (3, 4). On the other hand, Woo and colleagues suggested in their report that nonpneumonic SARS-CoV infections are more common than SARS pneumonia (24). Therefore, to clarify this, more-extensive seroprevalence studies are needed.

Currently, the most widely used serologic assays for SARS are indirect immunofluorescence assays using SARS-CoV-infected cells and enzyme-linked immunosorbent assays (ELISA) using cell culture extracts as antigens. In addition to causing antigenic cross-reactivity between SARS-CoV-infected Vero cells and group I coronaviruses, these methods are difficult and often cumbersome (10). Moreover, SARS-CoV-infected cells and cell culture extracts present a considerable risk of infection among laboratory workers. The frequent incidence

* Corresponding author. Mailing address: Department of Virology, Institute of Tropical Medicine, Nagasaki University, 1-12-4 Sakamoto, Nagasaki 852-8523, Japan. Phone: 81 95 849 7829. Fax: 81 95 849 7830. E-mail: moritak@net.nagasaki-u.ac.jp.

of SARS infections among laboratory researchers in Singapore, Taiwan, and Beijing, China, has caused great concern about laboratory safety (14, 27, 28). Hence, safer and more convenient methods for SARS diagnosis and large-scale epidemiological studies are needed.

The SARS outbreak in Vietnam began with the admission of a traveler from Hong Kong to the French Hospital, a 56-bed, three-story, privately owned, expatriate-operated hospital located in Hanoi, Vietnam, on 26 February 2003. Within 2 weeks, extensive nosocomial transmission of SARS occurred, mainly among the hospital staff. On 12 March, this hospital was closed to new admissions, with the exception of hospital workers. On 28 April 2003, Vietnam became the first country to recognize and contain a SARS outbreak, as announced by the WHO. In Vietnam, SARS occurred mainly in the above-mentioned French Hospital, among HCWs, and the existence of a clear index case transmitting the virus to close contacts was identified. All of these characteristics made this place ideal to study the epidemiology of this disease.

To undertake the study of SARS-CoV subclinical infection among Vietnamese HCWs, we developed a truncated SARS-CoV N protein-based ELISA system by using recombinant techniques. This new ELISA system is safer, more specific, and more sensitive for the diagnosis of SARS-CoV infection. The present study describes the existence of asymptomatic SARS-CoV infection in Vietnam, as proven by use of this new screening method and confirmed by a virus neutralization test. Data on the sensitivity and specificity of this SARS-CoV ELISA system based on recombinant truncated N proteins are discussed.

MATERIALS AND METHODS

Serum samples. One hundred seventy-five serum samples from healthy volunteers from Hanoi, collected before the SARS outbreak, were used as negative controls. Serum samples from 149 HCWs who were in close contact with SARS patients at the French Hospital in Hanoi were included in this study. Among them, 37 were probable SARS cases, per the WHO case definition, and 112 were symptom free. Serial serum samples from those 37 probable SARS cases and 112 symptom-free HCWs were collected from 11 March to 3 April 2003.

RNA extraction. SARS-CoV strain Hanoi 01-03, isolated from a Vietnamese patient, was propagated in a Vero E6 cell line maintained at 37°C in Eagle's minimum essential medium supplemented with 2% fetal calf serum and 0.2 mM of each nonessential amino acid for 4 days. Upon observation of 80 to 100% cytopathic effect (CPE), the infected culture supernatant was clarified by light centrifugation at 2,000 × g for 10 min. Viral RNA was extracted from 140 μl of infected culture supernatant by using the QIAamp viral RNA minikit (QIAGEN, Hilden, Germany) according to the manufacturer's instructions. The extracted RNA was eluted in 60 μl of elution buffer and then used as the template for reverse transcription (RT)-PCR.

Construction of recombinant plasmids. The gene for the SARS-CoV N protein was amplified by RT-PCR as previously described (9). PCR amplification was carried out using primers 5′-TAATGGATCCCAATCAAACCAA-3′ and 5′-TGTGGTCGACATGAGTGTTTAT-3′ to generate a gene for the N′ protein (the N protein with the four leading amino acids [aa] clipped) and primers 5′ AGAAGGATCCCTTCCCTACGGCGCT-3′ and 5′-TGTGGTCGACATGAG TGTTTAT-3′ to generate a gene for the $N\Delta_{121}$ protein (a second N protein construct with 121 aa of the N terminus truncated). The sense and reverse primers contained BamHI and SalI restriction sites (underlined), respectively. The 1.3-kb and 0.9-kb PCR-amplified DNA fragments were digested with BamHI and SalI and subsequently cloned into the corresponding restriction site of the pQE30 vector (QIAGEN, Hilden, Germany). Two expression products, one encompassing aa 5 to 422 and another encompassing aa 122 to 422 of the SARS-CoV N protein, were obtained, and both constructs contained a vector-derived His tag (histidine hexamer) at their N termini. The resultant recombinant proteins were designated SARS N′ and SARS $N\Delta_{121}$, respectively.

Expression and purification of the recombinant SARS-CoV N proteins. The recombinant SARS-CoV N proteins were expressed by inserting the recombinant plasmids containing the SARS-CoV N′ and SARS-CoV $N\Delta_{121}$ sequences into *Escherichia coli* strain XL1-Blue and then cultured at 30°C in Luria-Bertani medium containing 100 μg/ml of ampicillin. When the optical density at 600 nm (OD_{600}) of the culture reached 0.5, expression of the recombinant proteins was induced by the addition of 0.2 mM isopropyl-β-D-thiogalactopyranoside (IPTG) for 3 h. The cells were harvested by centrifugation, washed in phosphate-buffered saline (PBS) solution, resuspended in 10 mM PBS (pH 7.5)-500 mM NaCl, and frozen at −80°C. After being frozen and thawed three times, the cell suspension was sonicated for 2 min with an interval of 1 s between pulses and centrifuged at 30,000 × *g* for 15 min at 4°C. The supernatant was then applied to a Talon IMAC resin column (Clontech). After being washed with 10 mM PBS-500 mM NaCl containing 20 mM imidazole, the purified proteins were then eluted with 10 mM PBS (pH 7.5)-500 mM NaCl containing 250 mM imidazole. The protein solutions were aliquoted and stored in a final concentration of 10% glycerol at −80°C until use. Protein concentrations were determined by the Bradford method (1a) with a protein assay reagent kit (Bio-Rad), and the purity of the proteins was analyzed by sodium dodecyl sulfate-polyacrylamide gel electrophoresis (SDS-PAGE).

Western blot analysis. Western blotting was performed as described by Towbin et al. (21). Briefly, proteins separated in a 10% polyacrylamide gel were transferred to a polyvinylidene difluoride (PVDF) membrane (Immobilon; Millipore) by using a semidry electroblotter (Sartorius, Germany). The membrane was initially blocked with Blockace (Yukijirushi, Sapporo, Japan) overnight at 4°C; subjected to reaction with mouse antihistidine serum (1:200 dilution; Amersham Biosciences, NJ), SARS-CoV-immunized rabbit serum (1:200 dilution; supplied by the National Institute of Infectious Disease, Japan), or SARS patient serum (1:100 dilution) for 1 h at 37°C; and then incubated with rabbit anti-mouse immunoglobulin G (IgG)-peroxidase conjugate or goat anti-rabbit IgG–peroxidase conjugate or goat anti-human IgG–peroxidase conjugate (1:1,000 dilution) (all conjugates were procured from American Qualex, California) for 1 h at 37°C. Finally, the reaction results were visualized by dimethylamino benzidine (DAB) staining.

ELISA using the recombinant nucleocapsid proteins. A total of 175 serum samples collected from healthy volunteers in Vietnam before the SARS outbreak and 150 serial serum samples collected from 37 patients with pneumonia were used for the assessment of the IgG antibody ELISA. The optimal concentrations of recombinant N′ and $N\Delta_{121}$ proteins were determined by checkerboard titration with different dilutions of coating recombinant proteins. The optimal amount of antigen for plate coating was 0.13 μg per ELISA well for each recombinant protein. Ninety-six-well Nunc immunoplates (Roskilde, Denmark) were coated with recombinant N′ or $N\Delta_{121}$ protein antigens in carbonate buffer (pH 9.6) overnight at 4°C and then blocked with Blockace for 1 h at room temperature. After the immunoplates were washed six times with PBS-Tween 20, 100 μl of 1:100 human serum diluted in Blockace was added to each well and incubated for 1 h at 37°C. Then, after the plates were washed six times with PBS-Tween 20, 100 μl of 1:30,000-diluted horseradish peroxidase-conjugated goat anti-human IgG (American Qualex, California) was added to each well, and the plates were incubated at 37°C for 1 h. After six more washes with PBS-Tween 20, 100 μl of diluted *o*-phenylenediamine was added to each well and incubated in the dark at room temperature for 10 min. The reaction was then stopped by adding 100 μl of 1 N H_2SO_4 to each well. The OD_{492} for each well was measured with a 620-nm reference filter. Each sample was tested in duplicate, and the mean OD for each sample was calculated. ELISA titers were calculated from standardized reciprocal dilution values by using Thermo-Labsystem's Ascent photospectrometric data analysis software, version 2.6. Each serum sample was checked twice, and the mean antibody titers were recorded.

ELISA using SARS-CoV-infected cell lysates. An ELISA using SARS-CoV-infected Vero E6 cell lysates was performed according to the protocol of the Centers for Disease Control and Prevention, Atlanta, Georgia (10). The cell lysates of the SARS-CoV-infected and -uninfected Vero E6 cells were supplied by the Centers for Disease Control and Prevention.

Virus neutralization test. A virus neutralization test was done under biosafety level 3 conditions by using the 50% tissue culture infective dose method. Briefly, sera were heat inactivated at 56°C for 30 min and then serially diluted twofold from 1:10 to 1:1,280. An equal volume of virus-infected cell culture fluid with a titer of 200 50% tissue culture infective doses was added to 200 μl of each serum dilution and incubated for 1 h at 37°C. Each dilution was then added to triplicate wells on a 96-well culture plate with Vero E6 cells previously grown to confluence. After 5 days, the existence of CPE was determined and quantified. Neutralization titers were expressed as the reciprocal values of the highest dilution of serum for which a 50% reduction of CPE was observed.

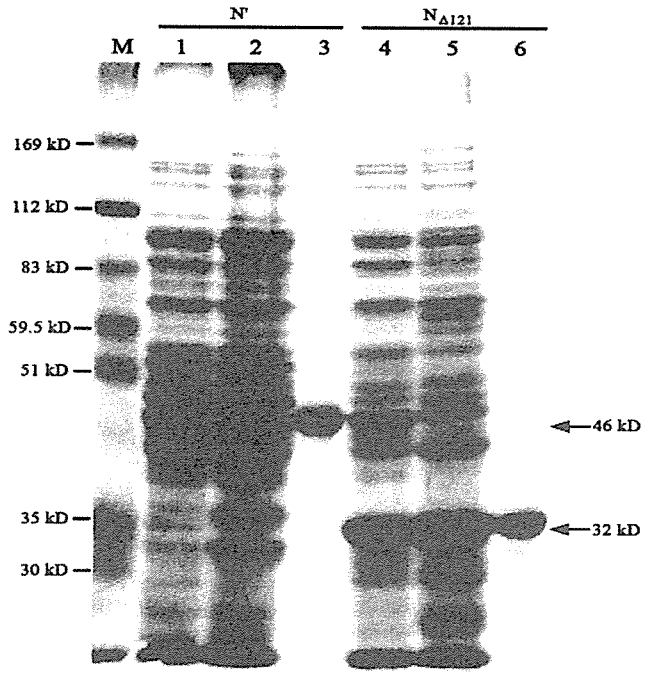

FIG. 1. Recombinant plasmids containing the N′ and $N\Delta_{121}$ genes were transformed into *E. coli* strain XL1-Blue and induced with IPTG. *E. coli* cell lysates were analyzed in a 10% SDS-PAGE gel and revealed with Coomassie brilliant blue staining. Lane M, protein marker (SDS-7B; Sigma, St. Louis, Mo.); lanes 1 and 4, supernatant of sonicated *E. coli* cell lysate after centrifugation; lanes 2 and 5, pellet of sonicated *E. coli* cell lysate; lanes 3 and 6, purified recombinant protein.

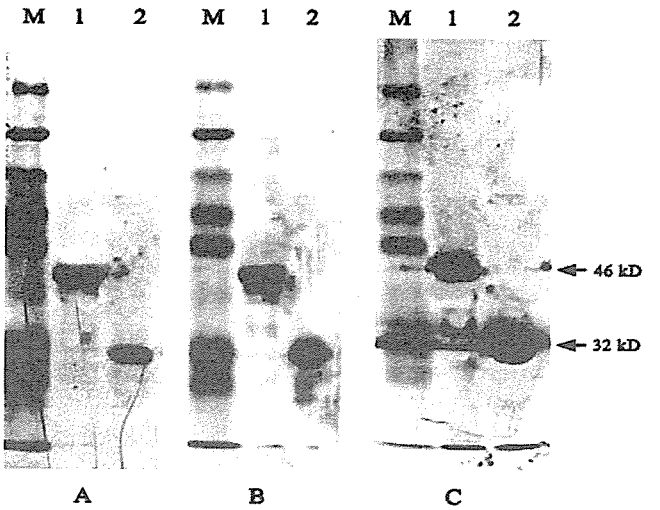

FIG. 2. Western blot analysis of purified N′ and $N\Delta_{121}$ proteins. The prestained protein marker and purified recombinant proteins were separated by SDS-PAGE and transferred to a PVDF membrane. Each membrane was incubated with diluted serum, followed by horseradish peroxidase-conjugated anti-rabbit IgG, anti-mouse IgG, or anti-human IgG (1:1,000 dilution), and detected by DAB staining. (A) Reactivity of recombinant proteins to rabbit anti-SARS-CoV serum. (B) Reactivity of recombinant proteins to mouse antihistidine serum. (C) Reactivity of recombinant proteins to SARS patient serum. Lanes M, protein marker (SDS-7B); lanes 1, purified SARS N′ protein; lanes 2, purified SARS $N\Delta_{121}$ protein.

RESULTS

Expression and purification of recombinant SARS-CoV N proteins. The recombinant SARS-CoV N proteins, encompassing amino acid residues 5 to 422 and 122 to 422 of the nucleocapsid protein, were amplified by RT-PCR and cloned into the BamHI and SalI sites of the expression vector pQE30 in frame and downstream of the six-histidine tag. The recombinant proteins were successfully expressed in *E. coli* and purified by use of a Talon metal affinity column under natural conditions. Analysis of purified recombinant proteins by SDS-PAGE and Coomassie blue staining revealed, as predicted, single protein bands of 46 kDa and 32 kDa for the two recombinant SARS-CoV N′ and $N\Delta_{121}$ proteins, respectively (Fig. 1). The identities of the recombinant SARS-CoV N′ and $N\Delta_{121}$ proteins were further confirmed by Western blot assay with mouse antihistidine serum, SARS-CoV-immunized rabbit serum, and SARS patient serum (Fig. 2).

Calibration of ELISA for recombinant N′ and $N\Delta_{121}$ proteins. In order to determine the basal titers and cutoff values, serum samples collected from 175 healthy volunteers in Vietnam before the SARS outbreak were used for the assessment of the indirect IgG ELISA for recombinant SARS-CoV N′ and SARS-CoV $N\Delta_{121}$ proteins. When the N′ protein was used as the coating antigen, 38 out of the 175 serum samples showed titers higher than 100, ranging from 100 to 3,200. On the contrary, when the SARS-CoV $N\Delta_{121}$ protein was used, only 11 out of 175 samples showed titers between 100 and 260. Further analysis of all of these positive samples by Western blotting also confirmed the reactivities (data not shown), indicating that the positive reaction by ELISA was not due to the potential interaction between residual *E. coli* antigens and naturally occurring antibodies against *E. coli* in human sera. We chose seven serum samples which showed high titers by the N′ protein-based ELISA but were negative by the $N\Delta_{121}$ protein-based ELISA and confirmed their reactivities by Western blot assay. As shown in Fig. 3, these seven samples were positive by the N′ protein-based Western blot assay but negative by the $N\Delta_{121}$ protein-based Western blot assay. This indicates

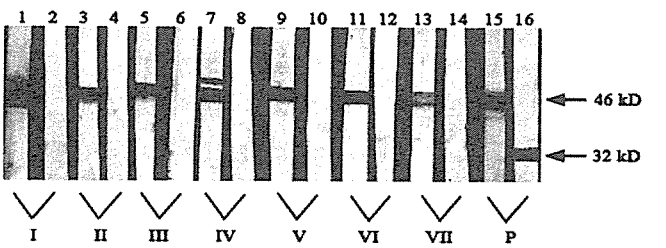

FIG. 3. Western blot analysis of sera that reacted with the N′ protein but not with the $N\Delta_{121}$ protein. Purified recombinant N′ and $N\Delta_{121}$ proteins were separated by SDS-PAGE and transferred to a PVDF membrane separately. The membranes were cut into strips and incubated with diluted serum (1:100 dilution) from seven healthy volunteers (I, II, III, IV, V, VI, and VII), followed by horseradish peroxidase-conjugated anti-human IgG (1:1,000 dilution), and detected by DAB staining. These sera showed high titers of antibodies to the N′ protein by the N′ protein-based ELISA but were negative by the $N\Delta_{121}$ protein-based ELISA. P, SARS patient serum used as a positive control. The odd-numbered lanes represent reactions with the N′ protein, and the even-numbered lanes represent reactions with the $N\Delta_{121}$ protein.

TABLE 1. Comparison of recombinant-$N_{\Delta 121}$ protein-based ELISA and SARS-CoV-infected cell lysate-based ELISA[a]

Method	No. (%[b]) of patients		Antibody titer of positive samples		Day of detection of seroconversion	
	IgG negative	IgG positive	Approx range	Geometric mean[c]	Earliest	Median[d]
$N_{\Delta 121}$-based ELISA	1	36 (97.3)	600–204,800	11,768	6	12
SARS-CoV-infected cell lysate-based ELISA	16	21 (56.8)	400–6,400	2,540	9	19

[a] Sera from 37 SARS patients were used.
[b] Positive rate at 3 weeks after onset of fever.
[c] For the 21 patient serum samples which were positive for IgG by both methods.
[d] For the 21 patient serum samples which were positive for IgG by both methods.

that the cross-reactivity observed for these healthy volunteer donors was caused by the N terminus of the SARS-CoV N protein, which has conserved motifs with other coronaviruses (18).

Evaluation of recombinant $N\Delta_{121}$ protein-based ELISA. Serial serum samples collected from 37 probable SARS cases were assessed by the recombinant $N\Delta_{121}$ protein-based ELISA to determine the presence of IgG antibodies to the SARS-CoV N protein. Thirty-six out of 37 patients (97.3%) showed specific IgG seroconversion, with titers ranging from 600 to 204,800. All positive samples were confirmed by Western blot assay. Among those 36 IgG-positive patients, anti-$N\Delta_{121}$ protein IgG seroconversion rates were 22.2%, 69.4%, and 100% within 7 days, 2 weeks, and 3 weeks after the onset of fever, respectively. One patient did not have detectable IgG antibodies to the $N\Delta_{121}$ protein. This patient's serum samples were collected only up to day 14 after the onset of disease; hence, a late seroconversion to SARS-CoV positivity might be the explanation for the lack of reaction. We also tested these patients' serum samples with the recombinant N′ protein-based ELISA and found that the reaction range and titers showed no difference from those obtained by the $N\Delta_{121}$ protein-based ELISA (data not shown).

In the recombinant $N\Delta_{121}$ protein-based IgG ELISA, the highest IgG titer observed for the group of 175 healthy volunteers was 260, and the lowest IgG titer observed for the SARS patients was 600. Therefore, 300 was set as the cutoff titer for our $N\Delta_{121}$ protein-based IgG ELISA. After the cutoff titer was set at 300, the clinical specificity of the $N\Delta_{121}$ protein-based IgG ELISA was 100%.

Comparison of recombinant $N\Delta_{121}$ protein-based ELISA with SARS-CoV-infected cell lysate-based ELISA. We compared the recombinant $N\Delta_{121}$ protein-based ELISA with the SARS-CoV-infected cell lysate-based ELISA by using serial serum samples collected from 37 probable SARS cases. As shown in Table 1, the recombinant $N\Delta_{121}$ protein-based ELISA showed a seroconversion rate of 97.3%, while that of the SARS-CoV-infected cell lysate-based ELISA was only 56.8%. The highest titers detected were 204,800 and 6,400, and the earliest seroconversion times detected after the onset of illness were 6 days and 9 days for the $N\Delta_{121}$ protein-based ELISA and the SARS-CoV-infected cell lysate-based ELISA, respectively. For the 21 samples that were positive by both methods, the $N\Delta_{121}$ protein-based ELISA detected seroconversion earlier than the SARS-CoV-infected cell lysate-based ELISA in 16 samples and on the same day for the other 5 samples. The median seroconversion times were 12 days and 19 days, and the geometric mean titers were 11,768 and 2,540 for the $N\Delta_{121}$ protein-based ELISA and the SARS-CoV-infected cell lysate-based ELISA, respectively.

Identification of inapparent SARS infection. Using the recombinant $N\Delta_{121}$ protein-based IgG ELISA, we screened serum samples collected from 112 symptom-free Vietnamese HCWs who had close contact with SARS patients. Four of those 112 HCWs had anti-SARS-CoV $N\Delta_{121}$ protein antibodies. Three of them, for whom paired samples were tested, showed IgG seroconversion, and the fourth one showed a titer of 8,400 for a single blood serum sample. All four cases were confirmed by Western blotting and neutralization tests. The neutralizing antibody titers observed for these four HCWs were 24, 48, 48, and 114, respectively. For the three individuals for whom paired serum samples were available, the first serum sample was negative by neutralization test. This clearly demonstrated that these four HCWs acquired inapparent SARS-CoV infections during the SARS outbreak. As shown in Table 2, out of 149 HCWs who were in close contact with SARS patients at the French Hospital, 37 (24.8%) had SARS and 4 (2.7%) experienced asymptomatic infection ($P < 0.001$), indicating the existence of a relatively low rate of inapparent SARS-CoV infection among HCWs in Vietnam.

DISCUSSION

There are several reports on the use of recombinant SARS-CoV nucleocapsid protein for the serodiagnosis of SARS-CoV clinical infection, indicating that SARS-CoV nucleocapsid protein is highly immunogenic and abundantly expressed during infection and is therefore useful for the diagnosis of SARS-CoV infection (5, 7, 20). Since the N proteins of known coronaviruses are relatively conserved, it is important to ascertain whether SARS-CoV N protein is cross-reactive with other coronaviruses and especially with antisera of other human coronaviruses. Sun and Meng reported that the N protein of SARS-CoV reacted strongly with polyclonal antisera of known antigenic group I coronaviruses, indicating that the SARS-CoV N protein shares a common antigenic epitope(s) with

TABLE 2. Rates of clinical and inapparent SARS-CoV infection in HCWs in Vietnam[a]

Symptom status	No. of HCWs positive for SARS/total no of HCWs (%)
SARS patient	37/149 (24.8)
Subclinical SARS infection	4/149 (2.7)

[a] A P value of <0.001 was determined by the χ^2 test.

animal coronaviruses belonging to antigenic group I (19). Woo et al. also reported that recombinant SARS-CoV nucleocapsid protein-based ELISA and Western blot assays have high rates of false positivity (24). In a recent report, Woo et al. found that 3 out of 21 and 1 out of 7 convalescent-phase serum samples from persons infected with human coronavirus (HCoV)-OC43 and HCoV-229E, respectively, tested positive by recombinant SARS-CoV nucleocapsid protein-based ELISA, suggesting that there is cross-reactivity between SARS-CoV N protein and HCoV-OC43 and HCoV-229E N proteins (25). It has been reported that antibodies against human 229E- and OC43-like coronaviruses are widespread within the human population (1, 16). Our recombinant SARS-CoV N′ protein-based ELISA revealed that 38 out of 175 serum samples from healthy volunteers collected before the SARS outbreak had titers higher than 100, ranging from 100 to 3,200. Taken together, these facts indicate that the reactivity we observed for the healthy volunteer sera presented in this study was probably due to cross-reactivity with existing antibodies to other circulating coronaviruses. This clearly indicates that care should be taken while interpreting assay results when the full-length recombinant N protein of SARS-CoV, whole-virus antigen extracts, or virus-infected cells are used as reagents for the diagnosis of SARS-CoV infections in humans and animal species.

The predicted N protein of SARS-CoV is a highly charged basic protein of 422 amino acids with seven successive hydrophobic residues near the middle of the protein. Although the overall amino acid sequence homology of the SARS-CoV N protein to other human coronaviruses is very low (32.7% between SARS-CoV and human coronavirus OC43 and 21.3% between SARS-CoV and human coronavirus 229E), a highly conserved motif (FYYLGTGP) occurs in the N-terminal half of all coronavirus N proteins, and other conserved residues are reported to occur near this highly conserved motif (18). Using synthetic peptides, Wang et al. found that the most immunoreactive epitopic site in the SARS coronavirus N protein is located at its COOH terminus (23). In theory, these findings made it possible to remove the N terminus of the SARS-CoV N protein, which contains the conserved motif of all coronavirus N proteins, to reduce cross-reactivity in SARS diagnosis. We expressed a truncated SARS-CoV $N\Delta_{121}$ protein, in which the highly conserved motif (FYYLGTGP) was deleted. When this $N\Delta_{121}$ protein was used as the coating antigen for our ELISA, 11 out of 175 samples showed weak reactions, with titers ranging from 100 to 260, much fewer positive samples with titers much lower than those observed when the N′ protein was used. This was confirmed by Western blot analysis (Fig. 3). Our results further supported the fact that the SARS-CoV N protein shows cross-reactivity with those of other coronaviruses and that such cross-reaction is caused by the conserved motif present within the N terminus of the protein. The fact that 11 samples also showed, although with low titers, reactivity against the SARS-CoV $N\Delta_{121}$ protein suggests that some minor common motifs might still exist within the truncated $N\Delta_{121}$ protein. Finally, to solve cross-reactivity problems, 300 was set as the cutoff titer, and all of these weak reactions were interpreted as negative in our ELISA system.

To assess the sensitivity of the $N\Delta_{121}$ protein-based IgG ELISA, serially collected serum samples from 37 probable SARS cases were examined. Thirty-six patients (97.3%) showed IgG seroconversion, and the serum titers ranged from 600 to 204,800. Among these 36 positive cases, the anti-$N\Delta_{121}$ protein IgG seroconversion rates after the onset of illness were 22.2% by the first week, 69.4% by the second week, and 100% by the third week. The recombinant $N\Delta_{121}$ protein-based ELISA was more sensitive and could detect seroconversion earlier than the virus-infected cell lysate-based ELISA system (Table 1). Our newly developed SARS-CoV $N\Delta_{121}$ protein-based IgG ELISA is a safe, specific, and sensitive test for the diagnosis of SARS-CoV infection. Therefore, it may be useful for clinical diagnosis and large-scale seroepidemiological studies.

Using the SARS-CoV $N\Delta_{121}$ protein-based IgG ELISA, we screened serum samples from 112 symptom-free HCWs who had direct contact with SARS patients in Vietnam. We found that four symptom-free HCWs had developed antibody against SARS-CoV. In addition, a positive reaction was confirmed by Western blotting and virus neutralization tests. This proved that all four symptom-free HCWs truly had subclinical SARS-CoV infections. The comparison of rates of symptomatic and asymptomatic SARS-CoV infections among HCWs in Vietnam revealed that symptomatic infection was more common than subclinical infection (Table 2). Therefore, our data strongly indicate that subclinical SARS-CoV infection actually does exist, although at quite a low rate.

Vietnam was the first country in which SARS was acknowledged. At the beginning of the outbreak, the severity of the disease was not recognized; hence, no effective prevention measures were taken. Therefore, within 2 weeks, extensive nosocomial transmission occurred among the hospital staff at the French Hospital. Contact-tracing data revealed that all of the four symptom-free HCWs from this study who had antibodies against SARS-CoV were in direct contact with the index case; however, they did not develop SARS but experienced only subclinical infection, as proven by seroconversion. There have been several reports dealing with subclinical or atypical forms of SARS. Lee et al. reported a case of possible asymptomatic SARS-CoV infection in Hong Kong (11). Li et al. reported that, among 125 people exposed to SARS patients, 20 developed SARS and 2 had nonpneumonic infections (13). In addition, Ho et al. reported that 8 out of 372 HCWs in a teaching hospital in Singapore were positive for SARS-CoV antibody. Among them, six were probable or suspected SARS cases; however, two had only fever, indicating that a small number of mildly symptomatic individuals existed, although no asymptomatic individuals were found (6). Chow et al. reported that with a dot blot ELISA combined with a virus neutralization test of 87 HCW serum samples, no subclinical SARS was found (4). In addition, Chan et al., using an indirect immunofluorescence assay, examined 674 HCWs from a hospital in which a SARS outbreak had occurred, and none of the HCWs had antibodies to SARS-CoV (3). In a later report, Ip et al. found that 3 out of 131 HCWs who worked in SARS medical wards had subclinical infections (8). All of these studies used inactivated virus-infected cell extract-based ELISA or virus-infected cell-based immunofluorescence assays for diagnosis; however, as shown in our study, the inactivated virus-infected cell extract-based ELISA detected SARS antibodies with low sensitivity. Besides, with these methods, the possibility of cross-reaction with other human coronaviruses exists. On the con-

trary, our detection system, which consists of a truncated N protein-based ELISA for the screening of symptom-free HCWs and confirmation by a virus neutralization test, is more sensitive and more specific, giving much more reliable results to elucidate subclinical SARS-CoV infection.

On the other hand, Woo and colleagues, using a recombinant N protein-based ELISA combined with Western blot analysis for the detection of SARS-CoV N and S proteins, found that 3 out of 400 healthy blood donors and 1 out of 131 nonpneumonic inpatients were positive for SARS-CoV antibodies. Therefore, they concluded that subclinical or nonpneumonic SARS-CoV infections are more common than SARS pneumonia (24). As suspected by other researchers, this could be due to cross-reactivity or misinterpretation of their results (29).

Considering all previously reported information and our data, it is clear that subclinical and mild forms of SARS-CoV infection are rare but existent. This may be the reason why control measures, such as quarantining patients, worked effectively to contain the outbreak in Vietnam. SARS-CoV was a newly emerged virus, and humans did not have immunity against it; as a result, most of the people infected developed clinically symptomatic infections. This implies that another outbreak could occur, because only very few people may have acquired immunity through subclinical infections and, hence, the majority of the population might remain susceptible to the disease.

In conclusion, we developed a SARS-CoV $N\Delta_{121}$ protein-based IgG ELISA which is a safe, specific, and sensitive test for the diagnosis of SARS-CoV infection. We also demonstrated that subclinical SARS-CoV infection, though rare, does indeed occur.

ACKNOWLEDGMENTS

This study was supported in part by a Grant for Research on Emerging and Reemerging Infectious Diseases (no. 16171001) from the Ministry of Health, Welfare and Labor of Japan and the 21st Century Centers of Excellence [COE] program on Global Strategies for Control of Tropical and Emerging Infectious Diseases at Nagasaki University.

We thank Shigeru Morikawa of the Department of Virology, National Institute of Infectious Disease, Tokyo, Japan, for generously providing the SARS virus-immunized rabbit serum and Manmohan Parida for his critical suggestions in preparing the manuscript.

REFERENCES

1. **Bradburne, A. F., and B. A. Somerset.** 1972. Coronative antibody titers in sera of healthy adults and experimentally infected volunteers. J. Hyg. **70:** 235–244.
1a. **Bradford, M. M.** 1976. A rapid and sensitive method for the quantitation of microgram quantities of protein utilizing the principle of protein-dye binding. Anal. Biochem. **72:**248–254.
2. **Centers for Disease Control and Prevention.** 2003. Outbreak of acute respiratory syndrome worldwide, 2003. Morb. Mortal. Wkly. Rep. **52:**226–228.
3. **Chan, P. K., M. Ip, K. C. Ng, C. W. Rickjason, A. Wu, N. Lee, T. H. Rainer, G. M. Joynt, J. J. Sung, and J. S. Tam.** 2003. Severe acute respiratory syndrome-associated coronavirus infection. Emerg. Infect. Dis. **9:**1453–1454.
4. **Chow, P. K., E. E. Ooi, H. K. Tan, K. W. Ong, B. K. Sil, M. Teo, T. Ng, and K. C. Soo.** 2004. Healthcare worker seroconversion in SARS outbreak. Emerg. Infect. Dis. **10:**249–250.
5. **Guan, M., H. Y. Chen, S. Y. Foo, Y.-J. Tan, P.-Y. Goh, and S. H. Wee.** 2004. Recombinant protein-based enzyme-linked immunosorbent assay and immunochromatographic tests for detection of immunoglobulin G antibodies to severe acute respiratory syndrome (SARS) coronavirus in SARS patients. Clin. Diagn. Lab. Immunol. **11:**287–291.
6. **Ho, K. Y., K. S. Singh, A. G. Habib, B. K. Ong, T. K. Lim, E. E. Ooi, B. K. Sil, A.-E. Ling, X. L. Bai, and P. A. Tambyah.** 2004. Mild illness associated with severe acute respiratory syndrome coronavirus infection: lessons from a prospective seroepidemiologic study of health-care workers in a teaching hospital in Singapore. J. Infect. Dis. **189:**642–647.
7. **Huang, L. R., C. M. Chiu, S. H. Yeh, W. H. Huang, P. R. Hsueh, W. Z. Yang, J. Y. Yang, I. J. Su, S. C. Chang, and P. J. Chen.** 2004. Evaluation of antibody responses against SARS coronaviral nucleocapsid or spike proteins by immunoblotting or ELISA. J. Med. Virol. **73:**338–346.
8. **Ip, M., P. K. S. Chan, N. Lee, A. Wu, T. K. C. Ng, L. Chan, A. Ng, H. M. Kwan, L. Tsang, I. Chu, J. L. K. Cheung, J. J. Y. Sung, and J. S. Tam.** 2004. Seroprevalence of antibody to severe acute respiratory syndrome (SARS)-associated coronavirus among health care workers in SARS and non-SARS medical wards. Clin. Infect. Dis. **38:**e116–e118.
9. **Khan, A. H., K. Morita, M. C. Parquet, F. Hasebe, E. G. M. Mathenge, and A. Igarashi.** 2002. Complete nucleotide sequence of chikungunya virus and evidence for an internal polyadenylation site. J. Gen. Virol. **83:**3075–3084.
10. **Ksiazek, T. G., D. Erdman, C. S. Goldsmith, S. R. Zaki, T. Peret, S. Emery, S. Tong, C. Urbani, J. A. Comer, W. Lim, P. E. Rollin, S. F. Dowell, A. E. Ling, C. D. Humphrey, W. J. Shieh, J. Guarner, C. D. Paddock, P. Rota, B. Fields, J. DeRisi, J. Y. Yang, N. Cox, J. M. Hughes, J. W. LeDuc, W. J. Bellini, L. J. Anderson, and the SARS Working Group.** 2003. A novel corona virus associated with severe acute respiratory syndrome. N. Engl. J. Med. **348:**1953–1966.
11. **Lee, H. K., E. Y. Tso, T. N. Chau, O. T. Tsang, K. W. Choi, and T. S. Lai.** 2003. Asymptomatic severe acute respiratory syndrome-associated coronavirus infection. Emerg. Infect. Dis. **9:**1491–1492.
12. **Lee, N., D. Hui, A. Wu, P. Chan, P. Cameron, G. M. Joynt, A. Ahuja, M. Y. Yung, C. B. Leung, K. F. To, S. F. Lui, C. C. Szeto, S. Chung, and J. J. Sung.** 2003. A major outbreak of severe acute respiratory syndrome in Hong Kong. N. Engl. J. Med. **348:**1986–1994.
13. **Li, G., X. Chen, and A. Xu.** 2003. Profile of specific antibodies to the SARS-associated coronavirus. N. Engl. J. Med. **349:**508–509.
14. **Lim, P. L., A. Kurup, G. Gopalakrishna, K. P. Chan, C. W. Wong, L. C. Ng, S. Y. Se-Thoe, L. Oon, X. Bai, L. W. Stanton, Y. Ruan, L. D. Miller, V. B. Vega, L. James, P. L. Ooi, C. S. Kai, S. J. Olsen, B. Ang, and Y. S. Leo.** 2004. Laboratory-acquired severe acute respiratory syndrome. N. Engl. J. Med. **350:**1740–1745.
15. **Marra, M. A., S. J. Jones, C. R. Astell, R. A. Holt, A. Brooks-Wilson, Y. S. Butterfield, J. Khattra, J. K. Asano, S. A. Barber, S. Y. Chan, A. Cloutier, S. M. Coughlin, D. Freeman, N. Girn, O. L. Griffith, S. R. Leach, M. Mayo, H. McDonald, S. B. Montgomery, P. K. Pandoh, A. S. Petrescu, A. G. Robertson, J. E. Schein, A. Siddiqui, D. E. Smailus, J. M. Stott, G. S. Yang, F. Plummer, A. Andonov, H. Artsob, N. Bastien, K. Bernard, T. F. Booth, D. Bowness, M. Drebot, L. Fernando, R. Flick, M. Garbutt, M. Gray, A. Grolla, S. Jones, H. Feldmann, A. Meyers, A. Kabani, Y. Li, S. Normand, U. Stroher, G. A. Tipples, S. Tyler, R. Vogrig, D. Ward, B. Watson, R. C. Brunham, M. Krajden, M. Petric, D. M. Skowronski, C. Upton, and R. L. Roper.** 2003. The genome sequence of the SARS-associated coronavirus. Science **300:**1399–1404.
16. **McIntosh, K., A. Z. Kapikian, H. C. Turner, J. W. Hartley, R. H. Parrott, and R. M. Ahanock.** 1970. Seroepidemiologic studies of coronavirus infection in adults and children. Am. J. Epidemiol. **91:**585–592.
17. **Poutanen, S. M., S. Finkelstein, R. Tellier, M. Ayers, D. Skowronski, A. S. Slutsky, and M. Petric.** 2003. Identification of severe acute respiratory syndrome in Canada. N. Engl. J. Med. **348:**1995–2005.
18. **Rota, P. A., M. S. Oberste, S. S. Monroe, W. A. Nix, R. Campagnoli, J. P. Icenogle, S. Peñaranda, B. Bankamp, K. Maher, M. Chen, S. Tong, A. Tamin, L. Lowe, M. Frace, J. L. DeRisi, Q. Chen, D. Wang, D. D. Erdman, T. C. T. Peret, C. Burns, T. G. Ksiazek, P. E. Rollin, A. Sanchez, S. Liffick, B. Holloway, J. Limor, K. McCaustland, M. Olsen-Rasmussen, R. Fouchier, S. Günther, A. D. M. E. Osterhaus, C. Drosten, M. A. Pallansch, L. J. Anderson, and W. J. Bellini.** 2003. Characterization of a novel coronavirus associated with severe acute respiratory syndrome. Science **300:**1394–1399.
19. **Sun, Z. F., and X. J. Meng.** 2004. Antigenic cross-reactivity between the nucleocapsid protein of severe acute respiratory syndrome (SARS) coronavirus and polyclonal antisera of antigenic group I animal coronaviruses: implication for SARS diagnosis. J. Clin. Microbiol. **42:**2351–2352.
20. **Timani, K. A., L. Ye, L. Ye, Y. Zhu, Z. Wu, and Z. Gong.** 2004. Cloning, sequencing, expression, and purification of SARS-associated coronavirus nucleocapsid protein for serodiagnosis of SARS. J. Clin. Virol. **30:**309–312.
21. **Towbin, H., T. Staehelin, and J. Gorden.** 1979. Electrophoretic transfer of proteins from polyacrylamide gels to nitrocellulose sheets: procedure and some applications. Proc. Natl. Acad. Sci. USA **76:**4350–4354.
22. **Tsang, K. W., P. L. Ho, G. C. Ooi, W. K. Yee, T. Wang, M. Chan-Yeung, W. K. Lam, W. H. Seto, L. Y. Yam, T. M. Cheung, P. C. Wong, B. Lam, M. S. Ip, J. Chan, K. Y. Yuen, and K. N. Lai.** 2003. A cluster of cases of severe acute respiratory syndrome in Hong Kong. N. Engl. J. Med. **348:**1977–1985.
23. **Wang, J., J. Wen, J. Li, J. Yin, Q. Zhu, H. Wang, Y. Yang, E. Qin, B. You, W. Li, X. Li, S. Huang, R. Yang, X. Zhang, L. Yang, T. Zhang, Y. Yin, X. Cui, X. Tang, L. Wang, B. He, L. Ma, T. Lei, C. Zeng, J. Fang, J. Yu, J. Wang, H. Yang, M. B. West, A. Bhatnagar, Y. Lu, N. Xu, and S. Liu.** 2003. Assessment of immunoreactive synthetic peptides from the structural proteins of severe acute respiratory syndrome coronavirus. Clin. Chem. **49:**1989–1996.

24. **Woo, P. C., S. K. Lau, H. W. Tsoi, K. H. Chan, B. H. Wong, X. Y. Che, V. K. Tam, S. C. Tam, V. C. Cheng, I. F. Hung, S. S. Wong, B. J. Zheng, Y. Guan, and K. Y. Yuen.** 2004. Relative rates of non-pneumonic SARS coronavirus infection and SARS coronavirus pneumonia. Lancet **363**:841–845.
25. **Woo, P. C. Y., S. K. P. Lau, B. H. L. Wong, K.-H. Chan, W.-T. Hui, G. S. W. Kwan, J. S. M. Peiris, R. B. Couch, and K.-Y. Yuen.** 2004. False-positive results in a recombinant severe acute respiratory syndrome-associated coronavirus (SARS-CoV) nucleocapsid enzyme-linked immunosorbent assay due to HCoV-OC43 and HCoV-229E rectified by Western blotting with recombinant SARS-CoV spike polypeptide. J. Clin. Microbiol. **42**:5885–5888.
26. **World Health Organization.** 2003. Severe acute respiratory syndrome (SARS). Wkly. Epidemiol. Rec. **78**:86–87.
27. **World Health Organization.** 2003. Severe acute respiratory syndrome (SARS) in Taiwan, China. [Online.] http://www.who.int/csr/don/2003_12_17/en/.
28. **World Health Organization.** 2004. China's latest SARS outbreak has been contained, but biosafety concerns remain—update 7. [Online.] http://www.who.int/csr/don/2004_05_18a/en/.
29. **Young, M., Y. H. Zhou, and M. Theron.** 2004. Prevalence of non-pneumonic infections with SARS-correlated virus. Lancet **363**:1825–1826. (Letter.)

Journal of General Virology (2005), 86, 2269–2274 DOI 10.1099/vir.0.80955-0

Short Communication

Vesicular stomatitis virus pseudotyped with severe acute respiratory syndrome coronavirus spike protein

Shuetsu Fukushi,[1] Tetsuya Mizutani,[1] Masayuki Saijo,[1] Shutoku Matsuyama,[2] Naoko Miyajima,[2] Fumihiro Taguchi,[2] Shigeyuki Itamura,[3] Ichiro Kurane[1] and Shigeru Morikawa[1]

Correspondence
Shuetsu Fukushi
fukushi@nih.go.jp

Special Pathogens Laboratory, Department of Virology I[1], Laboratory of Respiratory Viral Diseases and SARS[2] and Laboratory of Influenza Virus, Department of Virology III[3], National Institute of Infectious Diseases, Gakuen 4-7-1, Musashimurayama, Tokyo 208-0011, Japan

Severe acute respiratory syndrome coronavirus (SARS-CoV) contains a single spike (S) protein, which binds to its receptor, angiotensin-converting enzyme 2 (ACE2), induces membrane fusion and serves as a neutralizing antigen. A SARS-CoV-S protein-bearing vesicular stomatitis virus (VSV) pseudotype using the VSVΔG* system was generated. Partial deletion of the SARS-CoV-S protein cytoplasmic domain allowed efficient incorporation into VSV particles and led to the generation of a pseudotype (VSV-SARS-St19) at high titre. Green fluorescent protein expression was demonstrated as early as 7 h after infection of Vero E6 cells with VSV-SARS-St19. VSV-SARS-St19 was neutralized by anti-SARS-CoV antibody and soluble ACE2, and its infection was blocked by treatment of Vero E6 cells with anti-ACE2 antibody. These results indicated that VSV-SARS-St19 infection is mediated by SARS-CoV-S protein in an ACE2-dependent manner. VSV-SARS-St19 will be useful for analysing the function of SARS-CoV-S protein and for developing rapid methods of detecting neutralizing antibodies specific for SARS-CoV infection.

Received 9 February 2005
Accepted 21 April 2005

Severe acute respiratory syndrome (SARS) is a recently described infectious disease caused by a newly identified coronavirus, SARS-CoV (Drosten *et al.*, 2003; Ksiazek *et al.*, 2003). With a mortality rate of over 9 %, SARS has had major health and socio-economic impacts (Fouchier *et al.*, 2003). Despite intensive efforts, no effective antiviral treatments against SARS have yet been established. Studies of SARS-CoV infection have been limited because of the highly infectious nature of the virus and the problem of recent cases in which infection was suspected to have occurred in research laboratories.

Entry of SARS-CoV into susceptible cells is mediated by binding of the viral spike (S) protein to receptor molecules. The SARS-CoV-S protein has a 13 aa signal peptide at its N terminus, a single ectodomain of 1182 aa and a transmembrane region followed by a cytoplasmic domain of 28 aa (Marra *et al.*, 2003; Rota *et al.*, 2003). Recently, pseudotyped retroviruses bearing SARS-CoV-S protein have been generated by several laboratories (Hofmann *et al.*, 2004; Nie *et al.*, 2004; Simmons *et al.*, 2004). It has been shown that these pseudotyped viruses have a cell tropism identical to SARS-CoV and that their infection is dependent on a receptor molecule, angiotensin-converting enzyme 2 (ACE2), indicating that infection is mediated solely by SARS-CoV-S protein. Pseudotyped viruses provide a safe viral entry model because of their inability to produce infectious progeny virus. A quantitative assay of pseudotyped virus infection could facilitate research on SARS-CoV entry, cell tropism and neutralizing antibodies. Interestingly, it was reported that a pseudotyped retrovirus bearing a SARS-CoV-S protein variant with a truncation in the cytoplasmic domain was incorporated more efficiently into retrovirus particles than the full-length S protein (Giroglou *et al.*, 2004; Moore *et al.*, 2004).

Another pseudotyping system with a vesicular stomatitis virus (VSV) particle [the VSVΔG* system, in which the VSV G gene is replaced by the green fluorescent protein (GFP) gene] was reported previously to produce pseudotype VSV particles incorporating the envelope glycoproteins of several RNA viruses (i.e. measles virus, hantavirus, Ebola virus or hepatitis C virus; Matsuura *et al.*, 2001; Ogino *et al.*, 2003; Takada *et al.*, 1997; Tatsuo *et al.*, 2000). This system may be useful for research on viral envelope glycoproteins due to the ability of the pseudotype to grow at high titres in a variety of cell lines. The pseudotype virus titre obtained with the VSVΔG* system is generally higher than that of the pseudotype retrovirus system (Ogino *et al.*, 2003). Furthermore, infection of target cells with pseudotype VSV can be readily detected as GFP-positive cells by 16 h

Detection of expression of SARS-CoV-S protein and soluble mutated ACE2 are available as supplementary material in JGV Online.

post-infection (p.i.) because of the high level of GFP expression in the VSVΔG* system (Ogino *et al.*, 2003). In contrast, the time required for infection in the pseudotype retrovirus system is 48 h (Moore *et al.*, 2004; Nie *et al.*, 2004), which is similar to the time required for SARS-CoV to replicate to a level that results in plaque-forming or cytopathic effects in infected cells. To date, there have been no reports of VSV pseudotyped with the S protein of a coronavirus. Pseudotyping of SARS-CoV-S protein using the VSVΔG* system may have advantages for studying the functions of SARS-CoV-S protein, as well as for developing a rapid detection system to examine neutralizing antibodies specific for SARS-CoV infection.

To generate VSV pseudotyped with SARS-CoV-S protein, we first constructed an expression plasmid encoding full-length SARS-CoV-S protein. The cDNA of SARS-CoV-S protein was amplified using forward primer S-Bam-f (5′-GGATCCAAGTGATATTCTTGTTAACAAC-3′) and reverse primer S-Bam-r (5′-GGATCCAAGAGTAAAAAA-TCTCATAAAC-3′) and cloned into the expression vector pKS336 (Saijo *et al.*, 2002). The resulting plasmid, pKS-SARS-S, was transfected into 293T cells (see Supplementary Fig. S1, available in JGV Online), followed by infection with VSVΔG* (Matsuura *et al.*, 2001). When the culture supernatants of the infected 293T cells were inoculated on to Vero E6 cells, commonly used for SARS-CoV propagation, only small numbers of GFP-expressing cells were observed (data not shown). This result indicated that the VSV pseudotype bearing the full-length SARS-CoV-S protein was not very infectious. Next, we generated an expression plasmid encoding a C-terminal-truncated version of the SARS-CoV-S protein. The cDNA of C-terminal-truncated SARS-CoV-S protein was amplified from pKS-SARS-S using forward primer S-Bam-f and reverse primer S-Bam19r (5′-GGG-ATCCTTAGCAGCAAGAACCACAAGAGCATG-3′), followed by cloning into pKS336. The resulting plasmid, pKS-SARS-St19, encoded the full-length SARS-CoV-S protein except for the C-terminal 19 aa. When 293T cells were transfected with the expression plasmid pKS-SARS-St19, expression of the S protein was detected on the cell membrane (Supplementary Fig. S1). In contrast, transfection of the plasmid pKS-SARS-St19rev, in which the cDNA of C-terminal truncated SARS-CoV-S protein was inserted in the reverse orientation, did not show expression of SARS-CoV-S protein and was therefore used as a negative control for generating the VSV pseudotype. To generate a VSV pseudotype with the C-terminal truncated SARS-CoV-St19 protein, we inoculated VSVΔG* on to 293T cells transfected with either pKS-SARS-St19 or pKS-SARS-St19rev. VSVΔG*-G was used as a positive control, in which the deleted VSV-G protein was provided *in trans* encoded by pCAG-VSV-G (a kind gift from Dr Y. Matsuura, Osaka University, Japan) (Fig. 1a). The SARS-CoV-S protein-bearing VSV pseudotype, referred to as VSV-SARS-St19, obtained from 293T cells transfected with pKS-SARS-St19, efficiently infected Vero E6 cells (Fig. 1a). The titre of VSV-SARS-St19 was $5{\cdot}0 \times 10^5$ infectious units (IU) ml^{-1}. Since partial deletion of the SARS-CoV-S protein cytoplasmic domain allowed efficient incorporation into VSV particles and led to the generation of pseudotype at high titre, it was suggested that the intact cytoplasmic domain of SARS-CoV-S protein may have interrupted correct assembly of the pseudotype particles.

In order to confirm that the SARS-CoV-St19 protein was indeed incorporated into VSV particles, VSV pseudotypes were purified by ultracentrifugation using an RPS40T rotor (Hitachi) at 35 000 r.p.m. for 1 h through 20 % sucrose and then analysed by Western blotting using a rabbit antibody specific for aa 1124–1140 of SARS-CoV-S protein (Imgenex), a rabbit anti-VSV-G antibody (a kind gift from Dr S. Nagata, Tokyo University, Japan) and a mouse monoclonal antibody specific for VSV-M (a kind gift from Dr M. A. Whitt, GTx, Inc., TN, USA) (Fig. 1b). The VSV-M and SARS-CoV-S proteins were detected in VSV-SARS-St19, whereas the VSV-M and -G protein were detected in VSVΔG*-G. These results indicated that the SARS-CoV-St19 protein expressed in 293T cells was incorporated efficiently into VSV particles.

To determine the optimal incubation period for detection of VSV-SARS-St19 infection, we performed a time-course analysis of GFP expression. Vero E6 monolayers on 24-well glass slides were infected with VSV-SARS-St19. At various time points p.i., cells were photographed under a fluorescent microscope. The number of GFP-expressing cells in the photographs was counted using ImageJ software (http://rsb.info.nih.gov/ij/). Interestingly, GFP expression was detected clearly at 7 h p.i., although the fluorescence intensity of GFP expression was increased at 9 h p.i. (Fig. 1c). Infected cells detached from culture slides, presumably due to a cytopathic effect of VSV proteins, after incubation for 16 h (data not shown). As pseudoviruses are unable to produce progeny viruses, this system would be useful for the evaluation of cell entry mechanisms mediated by SARS-CoV-S protein. Therefore, the infection efficiency of VSV-SARS-St19 can be evaluated without incubation for up to 16 h p.i. Time-course analysis of the number of GFP-positive cells showed that quantification of VSV-SARS-St19 infection was possible at 7 h p.i. (Fig. 1c). Therefore, we counted the number of GFP-positive cells infected with VSV-SARS-St19 at 7 h p.i. for further study.

To confirm the specificity of infection, a rabbit anti-SARS-CoV antibody was tested for its ability to neutralize VSV-SARS-St19. The antibody was raised against UV-inactivated, purified SARS-CoV and reacted with SARS-CoV-S protein in an immunofluorescence assay (see Supplementary Fig. S1); the antibody showed neutralizing activity against SARS-CoV infection on Vero E6 cells at a dilution of 1 : 2560 (data not shown). As a negative control, we used a rabbit antibody raised against SARS-CoV-N protein-specific oligopeptides (Mizutani *et al.*, 2004). Culture medium containing 500 IU VSV-SARS-St19 was pre-incubated with serially diluted antibodies followed by inoculation on to Vero E6 cells. Pre-incubation with anti-SARS-CoV antibody showed

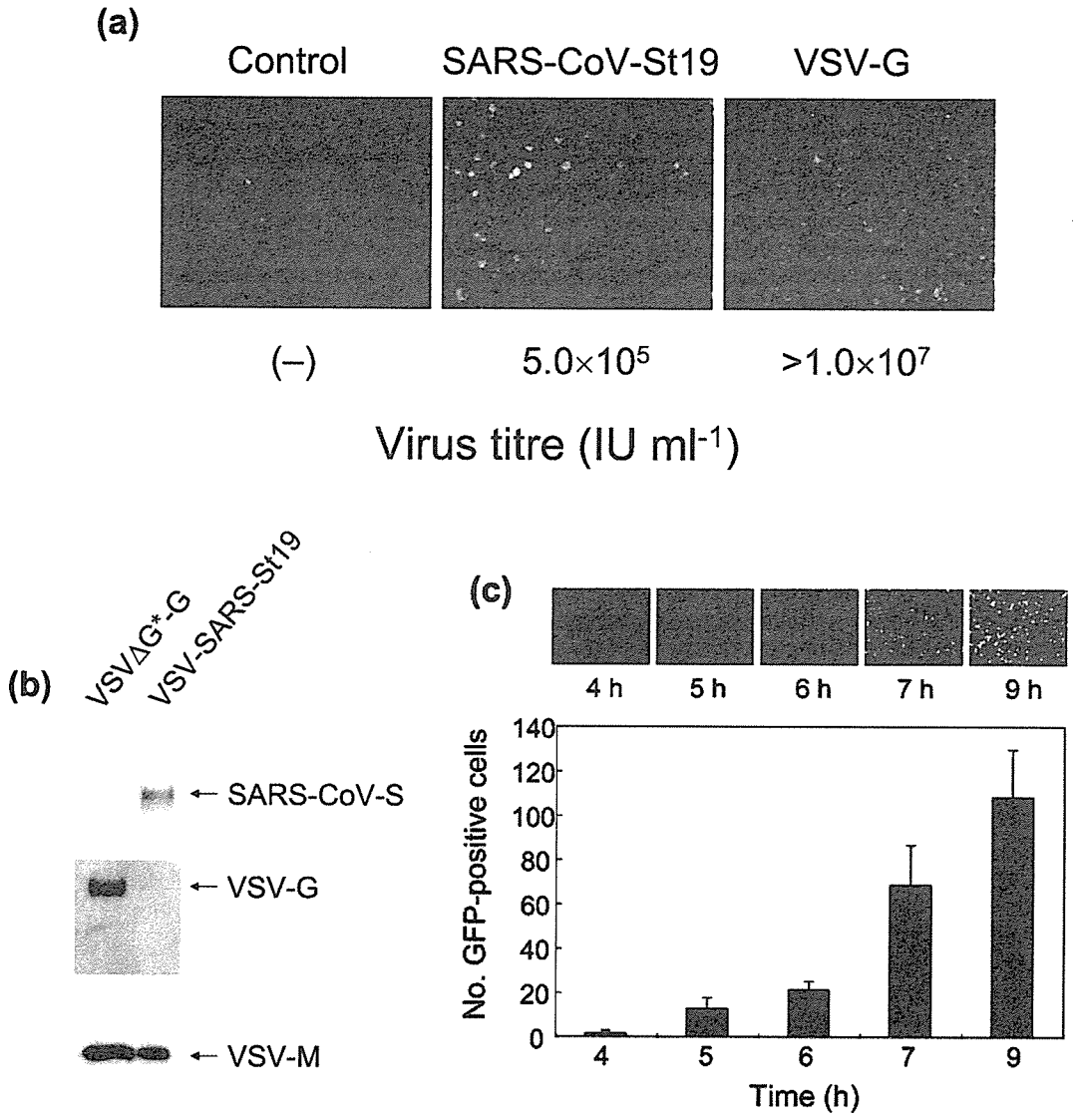

Fig. 1. Generation and characterization of VSV pseudotyped with SARS-CoV-S protein. (a) VSVΔG* was inoculated on to 293T cells expressing the indicated glycoproteins. After 24 h, culture supernatants were collected, filtered through a 0·22 μm pore size filter and inoculated on to Vero E6 cells. GFP expression was examined under a fluorescent microscope. The titre of pseudotypes viruses was determined by end-point dilution. (b) Incorporation of SARS-CoV-S protein into pseudotype VSV particles. VSV-SARS-St19 and VSVΔG*-G were partially purified by ultracentrifugation through 20 % sucrose. Viral proteins were analysed by Western blotting. The bands of SARS-CoV-S protein (180 kDa), VSV-G protein (62 kDa) and VSV-M protein (32 kDa) are indicated. (c) Rapid detection and quantification of VSV-SARS-St19 infection. Vero E6 cells were infected with VSV-SARS-St19 and GFP expression was examined at the indicated time points p.i. under a fluorescent microscope. The bar graph represents the number of GFP-positive cells per microscopic field (mean ± SD) calculated from six fields.

a significant reduction in the titre of VSV-SARS-St19 in a dose-dependent manner (Fig. 2a). Fifty per cent neutralizing activity was calculated at a dilution of 1:2000. In contrast, infection of Vero E6 cells with VSVΔG*-G was not affected by the anti-SARS-CoV antibody, even at a lower dilution (1:80 dilution) (Fig. 2a). When VSV-SARS-St19 was pre-incubated with control anti-SARS-CoV-N antibody, no neutralizing activity was observed (Fig. 2a). The possibility of carry-over of VSV-G during the production of VSV-SARS-St19, leading to infection of Vero E6 cells, was excluded, since an anti-VSV-G monoclonal antibody (P2F3, a kind gift from Dr. S. Nagata), which showed specific neutralizing activity against VSV infection (Nagata *et al.*, 1992), had no effect on infection of Vero E6 cells by VSV-SARS-St19 (Fig. 2b), but prohibited infection by VSVΔG*-G. These results indicated that infection of Vero E6 cells with

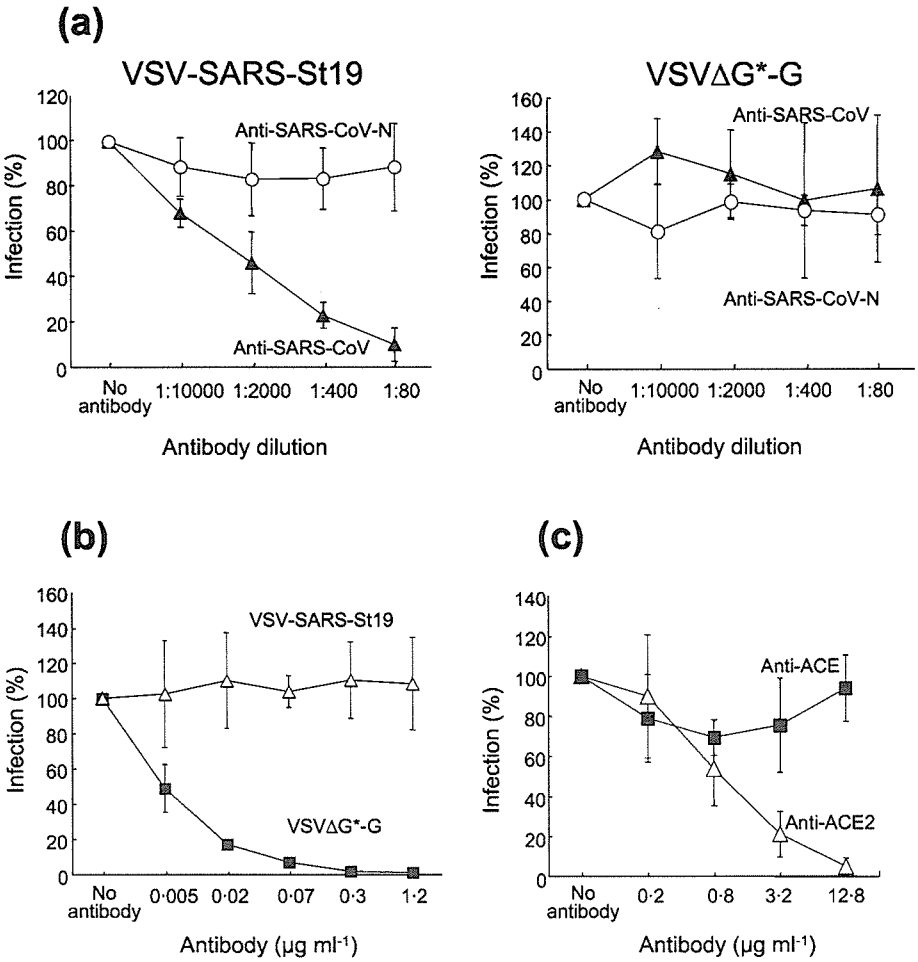

Fig. 2. Specificity of VSV-SARS-St19 pseudotype infection. (a) VSV-SARS-St19 (left) or VSVΔG*-G (right) was pre-incubated with serially diluted anti-SARS-CoV (▲) or anti-SARS-CoV-N (○) followed by inoculation on to Vero E6 cells. (b) VSV-SARS-St19 (△) or VSVΔG*-G (■) was pre-incubated with serially diluted anti-VSV-G antibody. (c) Vero E6 cells were pre-incubated with serially diluted anti-ACE (■) or anti-ACE2 (△) antibody and infected with VSV-SARS-St19. At 7 h p.i., GFP-positive cells were counted. The number of GFP-positive cells in the absence of antibodies was set as 100 %. The results are shown as mean ± SD for at least three independent assays.

VSV-SARS-St19 was mediated solely by SARS-CoV-S protein.

To determine whether anti-ACE2 antibody could inhibit VSV-SARS-St19 infection, Vero E6 cells were pre-incubated with anti-ACE2 antibody (R&D Systems) and the infectivity of VSV-SARS-St19 was examined. As a negative control, cells were pre-incubated with anti-ACE antibody (R&D Systems). As shown in Fig. 2(c), pre-incubation with anti-ACE2 antibody resulted in a significant reduction in VSV-SARS-St19 infection in a dose-dependent manner. Anti-ACE2 antibody, at a concentration of 12·8 μg ml^{-1}, completely inhibited VSV-SARS-St19 infection. In contrast, anti-ACE antibody had no appreciable effect on infection. These results indicated that VSV-SARS-St19 infection is ACE2-dependent. These observations were consistent with those reported previously by Li *et al.* (2003); on SARS-CoV infection of Vero E6 cells, the same polyclonal antibody showed an inhibitory effect on cytopathicity in a dose-dependent manner and complete inhibition was observed at an anti-ACE2 antibody concentration of approximately 10 μg ml^{-1}.

We further analysed whether soluble ACE2 protein could inhibit infection by VSV-SARS-St19. We introduced two amino acid substitutions at aa 374 and 378 within the putative catalytic domain of ACE2 (soACE2-NN; Supplementary Fig. S2). Purified soACE2-NN protein expressed in a baculovirus expression system was pre-incubated with VSV-SARS-St19 or VSVΔG*-G and the mixtures inoculated on to Vero E6 cells. As shown in Fig. 3(a), soluble ACE2 protein strongly inhibited VSV-SARS-St19 infection in a dose-dependent manner, but did not affect VSVΔG*-G infection. These observations indicated that purified soluble ACE2 specifically inhibited VSV-SARS-St19 infection. The highest concentration of soACE2 showed partial inhibition

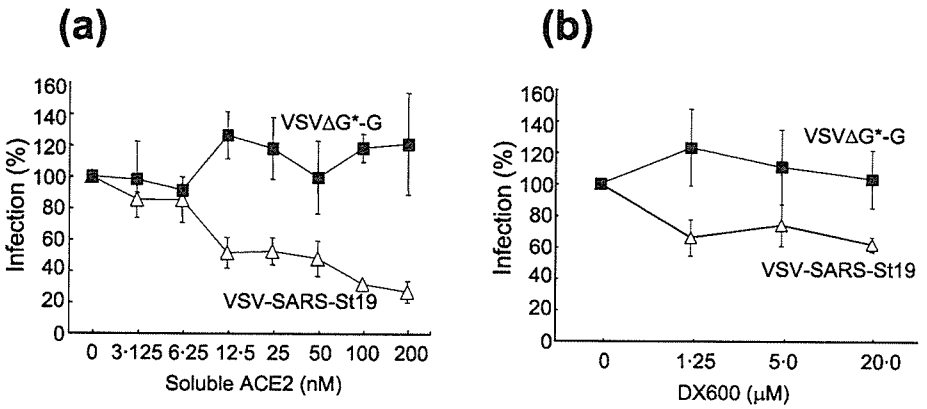

Fig. 3. Inhibition of VSV-SARS-St19 infection. VSV-SARS-St19 (△) or VSVΔG*-G (■) was pre-incubated with serially diluted soACE2NN (a) or DX600 (b), followed by inoculation on to Vero E6 cells. The infectivity of the pseudotypes was examined as described in Fig. 2.

(70–80 %) of VSV-SARS-St19 infectivity. However, the possibility that ACE2-independent entry of the pseudotype virus also existed could be excluded, since anti-ACE2 antibody completely inhibited VSV-SARS-St19 infectivity and almost all of the infection was dependent on ACE2 (Fig. 2c). The amount of soluble ACE2 that neutralized 50 % of the VSV-SARS-St19 infection (50 % neutralizing dose; ND_{50}) was estimated to be 12·5 nM. The neutralization activity of soACE2 in the present study was somewhat lower than that reported by Moore *et al.* (2004). This may have been due to the different strategies used for soACE2 preparation. The neutralization activity of soACE2 against SARS-CoV infection was lower than that of soluble mouse hepatitis virus receptor (soMHVR) against MHV infection (ND_{50} = 1 nM; Miura *et al.*, 2004; Zelus *et al.*, 1998). These observations suggested that SARS-CoV infection is regulated less strictly by the receptor function than MHV infection. Alternatively, a subdomain of ACE2 protein might represent increasing neutralization activity if bound to the SARS-CoV-S protein more strongly than the full-length protein. Indeed, neutralization of MHV-A59 infection was enhanced when the N-terminal subdomain of MHVR was used for neutralization experiments (Zelus *et al.*, 1998). It is noteworthy that an alternative splice variant of mouse ACE2 mRNA, consisting of the 5′ half of mouse ACE2 mRNA and not containing the metalloproteinase catalytic domain, has been reported (Komatsu *et al.*, 2002).

We then investigated whether a known ACE2-specific peptide inhibitor competed against ACE2-mediated pseudotype virus infection. VSV-SARS-St19 was pre-incubated with various concentrations of DX600 (Phoenix Pharmaceuticals), which has been shown to bind to and inhibit the enzymic activity of ACE2 (Huang *et al.*, 2003), and the mixture was then inoculated on to Vero E6 cells. Interestingly, DX600 inhibited VSV-SARS-St19 infection, but did not inhibit VSVΔG*-G infection. Higher concentrations (>1·25 μM) of DX600 were required for 30–40 % inhibition, indicating that this inhibition was weak (Fig. 3b). It has been shown that enzymic activity is not required for ACE2 protein as a SARS-CoV receptor (Li *et al.*, 2003). However, our results indicated that incubation of DX600 partially influenced the ACE2 function as a SARS-CoV receptor. Further investigation including inhibition studies with live SARS-CoV will be needed to elucidate the efficacy of DX600. Our results suggest that ACE2-binding peptides can be used as specific inhibitors of SARS-CoV-S protein-mediated infection. Based on the results of neutralization experiments using anti-SARS-CoV antibody and anti-ACE2 antibody, we conclude that VSV-SARS-St19 infection of target cells is mediated by SARS-CoV-S protein. The assay system described here would be useful not only for developing a safe and rapid method of detecting neutralizing antibodies to SARS-CoV, but also for screening of inhibitors of SARS-CoV-S protein-mediated infection.

Acknowledgements

We thank Dr M. A. Whitt for providing the VSVΔG* and anti-VSV-M antibody, Dr S. Nagata for providing monoclonal antibody P2F3 and rabbit anti-VSV G antibody, and Dr Y. Matsuura for providing pCAG-VSVG. We also thank Ms M. Ogata for her assistance. This work was supported in part by a grant-in-aid from the Ministry of Health, Labor and Welfare of Japan and the Japan Health Science Foundation, Tokyo, Japan.

References

Drosten, C., Gunther, S., Preiser, W. & 23 other authors (2003). Identification of a novel coronavirus in patients with severe acute respiratory syndrome. *N Engl J Med* **348**, 1967–1976.

Fouchier, R. A., Kuiken, T., Schutten, M. & 7 other authors (2003). Aetiology: Koch's postulates fulfilled for SARS virus. *Nature* **423**, 240.

Giroglou, T., Cinatl, J., Jr, Rabenau, H., Drosten, C., Schwalbe, H., Doerr, H. W. & von Laer, D. (2004). Retroviral vectors pseudotyped with severe acute respiratory syndrome coronavirus S protein. *J Virol* **78**, 9007–9015.

Hofmann, H., Geier, M., Marzi, A., Krumbiegel, M., Peipp, M., Fey, G. H., Gramberg, T. & Pohlmann, S. (2004). Susceptibility to SARS coronavirus S protein-driven infection correlates with expression of angiotensin converting enzyme 2 and infection can be blocked by soluble receptor. *Biochem Biophys Res Commun* **319**, 1216–1221.

Huang, L., Sexton, D. J., Skogerson, K. & 13 other authors (2003). Novel peptide inhibitors of angiotensin-converting enzyme 2. *J Biol Chem* **278**, 15532–15540.

Komatsu, T., Suzuki, Y., Imai, J., Sugano, S., Hida, M., Tanigami, A., Muroi, S., Yamada, Y. & Hanaoka, K. (2002). Molecular cloning, mRNA expression and chromosomal localization of mouse angiotensin-converting enzyme-related carboxypeptidase (mACE2). *DNA Seq* **13**, 217–220.

Ksiazek, T. G., Erdman, D., Goldsmith, C. S. & 23 other authors (2003). A novel coronavirus associated with severe acute respiratory syndrome. *N Engl J Med* **348**, 1953–1966.

Li, W., Moore, M. J., Vasilieva, N. & 9 other authors (2003). Angiotensin-converting enzyme 2 is a functional receptor for the SARS coronavirus. *Nature* **426**, 450–454.

Marra, M. A., Jones, S. J., Astell, C. R. & 56 other authors (2003). The genome sequence of the SARS-associated coronavirus. *Science* **300**, 1399–1404.

Matsuura, Y., Tani, H., Suzuki, K. & 8 other authors (2001). Characterization of pseudotype VSV possessing HCV envelope proteins. *Virology* **286**, 263–275.

Miura, H. S., Nakagaki, K. & Taguchi, F. (2004). N-terminal domain of the murine coronavirus receptor CEACAM1 is responsible for fusogenic activation and conformational changes of the spike protein. *J Virol* **78**, 216–223.

Mizutani, T., Fukushi, S., Saijo, M., Kurane, I. & Morikawa, S. (2004). Phosphorylation of p38 MAPK and its downstream targets in SARS coronavirus-infected cells. *Biochem Biophys Res Commun* **319**, 1228–1234.

Moore, M. J., Dorfman, T., Li, W. & 9 other authors (2004). Retroviruses pseudotyped with the severe acute respiratory syndrome coronavirus spike protein efficiently infect cells expressing angiotensin-converting enzyme 2. *J Virol* **78**, 10628–10635.

Nagata, S., Okamoto, Y., Inoue, T., Ueno, Y., Kurata, T. & Chiba, J. (1992). Identification of epitopes associated with different biological activities on the glycoprotein of vesicular stomatitis virus by use of monoclonal antibodies. *Arch Virol* **127**, 153–168.

Nie, Y., Wang, P., Shi, X. & 13 other authors (2004). Highly infectious SARS-CoV pseudotyped virus reveals the cell tropism and its correlation with receptor expression. *Biochem Biophys Res Commun* **321**, 994–1000.

Ogino, M., Ebihara, H., Lee, B. H., Araki, K., Lundkvist, A., Kawaoka, Y., Yoshimatsu, K. & Arikawa, J. (2003). Use of vesicular stomatitis virus pseudotypes bearing Hantaan or Seoul virus envelope proteins in a rapid and safe neutralization test. *Clin Diagn Lab Immunol* **10**, 154–160.

Rota, P. A., Oberste, M. S., Monroe, S. S. & 32 other authors (2003). Characterization of a novel coronavirus associated with severe acute respiratory syndrome. *Science* **300**, 1394–1399.

Saijo, M., Qing, T., Niikura, M., Maeda, A., Ikegami, T., Sakai, K., Prehaud, C., Kurane, I. & Morikawa, S. (2002). Immunofluorescence technique using HeLa cells expressing recombinant nucleoprotein for detection of immunoglobulin G antibodies to Crimean-Congo hemorrhagic fever virus. *J Clin Microbiol* **40**, 372–375.

Simmons, G., Reeves, J. D., Rennekamp, A. J., Amberg, S. M., Piefer, A. J. & Bates, P. (2004). Characterization of severe acute respiratory syndrome-associated coronavirus (SARS-CoV) spike glycoprotein-mediated viral entry. *Proc Natl Acad Sci U S A* **101**, 4240–4245.

Takada, A., Robison, C., Goto, H., Sanchez, A., Murti, K. G., Whitt, M. A. & Kawaoka, Y. (1997). A system for functional analysis of Ebola virus glycoprotein. *Proc Natl Acad Sci U S A* **94**, 14764–14769.

Tatsuo, H., Okuma, K., Tanaka, K., Ono, N., Minagawa, H., Takade, A., Matsuura, Y. & Yanagi, Y. (2000). Virus entry is a major determinant of cell tropism of Edmonston and wild-type strains of measles virus as revealed by vesicular stomatitis virus pseudotypes bearing their envelope proteins. *J Virol* **74**, 4139–4145.

Zelus, B. D., Wessner, D. R., Williams, R. K., Pensiero, M. N., Phibbs, F. T., deSouza, M., Dveksler, G. S. & Holmes, K. V. (1998). Purified, soluble recombinant mouse hepatitis virus receptor, $Bgp1^b$, and Bgp2 murine coronavirus receptors differ in mouse hepatitis virus binding and neutralizing activities. *J Virol* **72**, 7237–7244.

JOURNAL OF VIROLOGY, Mar. 2005, p. 3639–3652
0022-538X/05/$08.00+0 doi:10.1128/JVI.79.6.3639–3652.2005

Vol. 79, No. 6

Ligand-Directed Gene Targeting to Mammalian Cells by Pseudotype Baculoviruses†

Yoshinori Kitagawa, Hideki Tani, Chang Kwang Limn, Tomoko M. Matsunaga, Kohji Moriishi, and Yoshiharu Matsuura*

Research Center for Emerging Infectious Diseases, Research Institute for Microbial Diseases, Osaka University, Osaka, Japan

Received 27 August 2004/Accepted 25 October 2004

The baculovirus *Autographa californica* multiple nucleopolyhedrovirus (AcMNPV) can infect a variety of mammalian cells, as well as insect cells, facilitating its use as a viral vector for gene delivery into mammalian cells. Glycoprotein gp64, a major component of the budded AcMNPV envelope, is involved in viral entry into cells by receptor-mediated endocytosis and subsequent membrane fusion. We examined the potential production of pseudotype baculovirus particles transiently carrying ligands of interest in place of gp64 as a method of ligand-directed gene delivery into target cells. During amplification of a gp64-null pseudotype baculovirus carrying a green fluorescent protein gene in gp64-expressing insect cells, however, we observed the high-frequency appearance of a replication-competent virus incorporating the gp64 gene into the viral genome. To avoid generation of replication-competent revertants, we prepared pseudotype baculoviruses by transfection with recombinant bacmids without further amplification in the gp64-expressing cells. We constructed gp64-null recombinant bacmids carrying cDNAs encoding either vesicular stomatitis virus G protein (VSVG) or measles virus receptors (CD46 or SLAM). The VSVG pseudotype baculovirus efficiently transduced a reporter gene into a variety of mammalian cell lines, while CD46 and SLAM pseudotype baculoviruses allowed ligand-receptor-directed reporter gene transduction into target cells expressing measles virus envelope glycoproteins. Gene transduction mediated by the pseudotype baculoviruses could be inhibited by pretreatment with specific antibodies. These results indicate the possible application of pseudotype baculoviruses in ligand-directed gene delivery into target cells.

The baculovirus *Autographa californica* multiple nucleopolyhedrovirus (AcMNPV) is an insect virus possessing a 134-kb double-stranded circular DNA genome (3). Due to the strong polyhedrin and p10 promoters, baculovirus is commonly used as a tool for the large-scale production of recombinant protein in insect cells (32, 38). Baculovirus is also capable of entering into a variety of mammalian cells to facilitate the expression of foreign genes under the control of the mammalian promoters without replication of the viral genome (8, 21, 61). Therefore, baculovirus is a useful viral vector, not only for the abundant expression of foreign genes in insect cells, but also for efficient gene delivery to mammalian cells (29). AcMNPV has a number of unique beneficial properties as a viral vector, including a large capacity for foreign gene incorporation, easy manipulation, and replication competence in insect cells combined with incompetence in mammalian cells. Therefore, the possibility of generating replication-competent revertants expressing baculoviral gene products, which can often lead to harmful immune responses against mammalian cells, is significantly lower than for other viral vectors presently in use. Furthermore, studies of host responses to baculovirus infection in vivo revealed that AcMNPV can stimulate interferon production in mammalian cell lines, conferring protection from lethal encephalomyocarditis virus infections in mice (18). Intranasal inoculation with AcMNPV also induces a strong innate immune response, protecting mice from lethal challenges of influenza A or B virus (1). The precise mechanism of protective immune response induction by AcMNPV, however, remains unclear.

Recently, several groups have reported enhanced gene transfer in a variety of cell lines infected with recombinant baculoviruses expressing either foreign viral envelope proteins, such as vesicular stomatitis virus envelope G protein (VSVG), or excess amounts of the endogenous envelope glycoprotein, gp64, on the virion surface (4, 65, 66). Although modification of the virion surface enhances the efficiency of gene transduction into a variety of cell lines, the utility of recombinant baculoviruses in cell-type-specific gene transduction is still unsatisfactory. Ojala et al. demonstrated that, while baculoviruses bearing either a single chain antibody fragment specific for carcinoembryonic antigen or a synthetic immunoglobulin G (IgG) binding domain derived from protein A could specifically bind target cells, cell type-specific gene transduction was unsuccessful (44, 45). Although gp64-null pseudotype baculoviruses expressing a foreign viral envelope protein, such as VSVG or fusion envelope glycoproteins from other baculoviruses, exhibited high infectivity to insect cells, their capacity for gene transduction into mammalian cells has yet to be explored (33, 34). The inefficiency of present gene transfer vectors in gaining entry into cells needing treatment can be problematic, as many therapeutic genes may be deleterious if delivered to bystander cells. Therefore, the development of a ligand-directed gene delivery vector capable of distinguishing between

* Corresponding author. Mailing address: Research Center for Emerging Infectious Diseases, Research Institute for Microbial Diseases, Osaka University, Osaka 565-0871, Japan. Phone: 81-6-6879-8340. Fax: 81-6-6879-8269. E-mail: matsuura@biken.osaka-u.ac.jp.

† This study is dedicated to the memory of Ikuko Yanase

target and nontarget tissue is essential for both the safety and efficacy of gene therapy.

In this study, we examined the stability of a generated gp64-null pseudotype baculovirus possessing the green fluorescent protein (GFP) gene during passages in insect cells stably expressing the gp64 protein. Replication-competent revertant viruses emerged with high frequency during passage in the cell line, incorporating the gp64 gene into the revertants' viral genomes. To overcome the emergence of revertant viruses during passage, we generated recombinant bacmids lacking the gp64 gene and carrying a ligand of interest and a reporter gene under the control of the polyhedrin and the CAG promoters, respectively. Pseudotype baculoviruses generated from these bacmids exhibited specific ligand-directed gene delivery into target cells. These pseudotype baculovirus vectors may be useful in future clinical gene targeting.

MATERIALS AND METHODS

Cells. *Spodoptera frugiperda* (Sf9) cells were grown in TC-100 medium (Sigma, St. Louis, Mo.) supplemented with 0.26% tryptose phosphate broth (Difco, Detroit, Mich.) and 10% (vol/vol) fetal bovine serum (FBS) (Sigma) (66). To establish a cell line constitutively expressing gp64, Sf9 cells were transfected with pAFgp64 (see below) and pIB/V5-His (Invitrogen, Carlsbad, Calif.) using UniFector reagent (B-Bridge, Sunnyvale, Calif.). Thirty-six hours after transfection, Sf9 cells were selected in TC-100 medium containing blasticidin (50 μg/ml; Invitrogen). Resistant cells were stained with anti-gp64 antibodies (AcV1) (kindly provided by P. Faulkner) (22); positive cells were sorted using a FACSCalibur (Becton Dickinson, Franklin Lakes, N.J.) to establish a cell line, Sfgp64, stably expressing gp64 at the cell surface. The human embryonic kidney cell line 293T and the hamster kidney cell line BHK, purchased from the American Type Culture Collection, were maintained in Dulbecco's modified Eagle's medium (Sigma) containing 2 mM L-glutamine, penicillin (50 IU/ml), streptomycin (50 μg/ml), and 10% FBS (66).

Construction of plasmids. We constructed two expression plasmids, pAF-MCS1 and pAF-MCS2, harboring the A3 actin promoter, a multiple cloning site, and the polyadenylation signal derived from the *Bombyx mori* fibroin H-chain gene, for the subcloning of ligand molecules. First, the promoter and polyadenylation signal were excised from pA3Fb-Luc, kindly provided by H. Bando (Hokkaido University, Sapporo, Japan), and inserted into pUC18. To generate pAFgp64, the gp64 gene was excised from pFBgp64 (see below) by digestion with SalI and HindIII. This fragment was then inserted into the SalI-HindIII site of pAF-MCS1. Recombinant baculoviruses were constructed using the transfer vector pFASTBAC1 (Invitrogen). To measure the expression of foreign genes in mammalian cells, the firefly luciferase gene under the control of the CAG promoter (43) was subcloned into pFASTBAC1. To construct the transfer vector pFBCAluc, the CAG-luciferase cassette was excised from pCAGluc (61) by digestion with SalI, extension with Klenow enzyme, and redigestion with BamHI and inserted into the SnaBI-BamHI site of pFASTBAC1.

pUCgp64locus was generated by cloning the EcoRI-SmaI fragment from AcMNPV genomic DNA (corresponding to 107,325 to 112,041 nt) (3) into the EcoRI-SmaI site of pUC18. To generate pUCgp64, a fragment encoding the gp64 gene was excised from pUCgp64locus by digestion with SpeI and BglII and then cloned into the XbaI-BamHI site of pUC18. The gp64 gene was excised from pUCgp64 by digestion with SalI and KpnI and inserted into the SalI-KpnI site of pFASTBAC1. The resulting plasmid was designated pFBgp64. To generate pFBgp64CAluc, the cassette including the polyhedrin promoter and the gp64 gene was excised from pFBgp64 by digestion with SnaBI and KpnI and cloned into pFBCAluc, which was digested with SalI, extended with Klenow enzyme, and redigested with KpnI. The VSVG gene fragment was excised from pCAG-VSVG (64) by digestion with EcoRI and cloned into the EcoRI site of pFASTBAC1 to create pFBVSVG. pFBGFP was constructed by excision of the GFP gene from pAcVSVG-CAGFP (65) by digestion with EcoRI and subsequent insertion into the EcoRI site of pFASTBAC1. To generate pFBVSVGCAluc and pFBGFPCAluc, the DNA fragment encoding the polyhedrin promoter and either the VSVG or GFP gene was excised from pFBVSVG or pFBGFP, respectively, by digestion with SnaBI and XhoI and cloned into pFBCAluc, which was digested with SalI, extended with Klenow enzyme, and redigested with XhoI.

cDNAs encoding human CD46 and signaling lymphocyte activation molecule (SLAM; also known as CDw150) were amplified from the genomic DNAs of CHO/CD46 (kindly provided by T. Seya) (25) and CHO.SLAM (kindly provided by Y. Yanagi) (67) cells, respectively, by PCR. The CD46-Fw (1st) (5′-TTTCCTCCGGAGAAATAACAGC-3′) and CD46-Rv (1st) (5′-CTAAGCCACAGTTGCACTCATG-3′) primers were used to amplify CD46 cDNA, and the SLAM-Fw (1st) (5′-TGACACGAAGCTTGCTTCTG-3′) and SLAM-Rv (1st) (5′-GTCGACCTTTGTTGGTCTCTGGTG-3′) primers were used to amplify SLAM cDNA. These PCR products were used as templates for a second PCR with the primers CD46-Fw-*Hind*III (5′-CCCCAAGCTTCCGCGCCGCGCATGGG-3′) and CD46-Rv-*Sal*I (5′-TTTTGTCGACTCAGCCTCTCTGCTCTGCTG-3′) to amplify CD46 cDNA and SLAM-Fw-*Hind*III (5′-CCCCAAGCTTCCTCATTGGCTGATGGATC-3′) and SLAM-Rv-*Sal*I (5′-AAAAGTCGACTCAGCTCTCTGGAAGTGTCA-3′) to amplify SLAM cDNA. The amplified CD46 and SLAM cDNAs were digested with HindIII and SalI and then cloned into the HindIII-SalI sites of pAF-MCS2 to create pAFCD46 and pAFSLAM, respectively. The CD46 and SLAM cDNAs were excised from pAFCD46 and pAFSLAM, respectively, by digestion with HindIII, extension with Klenow enzyme, and redigestion with XbaI and cloned into pFASTBAC1. To generate pFBCD46CAluc and pFBSLAMCAluc, the DNA fragments encoding the polyhedrin promoter and either the CD46 gene or the SLAM gene were excised from pFBCD46 or pFBSLAM, respectively, by digestion with SnaBI and PvuI and cloned into pFBCAluc. A mutant SLAM gene, SLAMcyto7, possessing a truncated cytoplasmic domain of 7 amino acids, was generated by PCR with the primers SLAM-Fw-SmaI (5′-CCCCCCGGGCCTCATTGGCTGATGGATC-3′) and SLAM-7aa-stop-Rv-*Sal*I (5′-GGGGGGTCGACTCAGTTCGTTTTACCTCTTCTTCTCAAC-3′). This PCR product was digested with SmaI and SalI and then cloned into the SmaI-SalI sites of pAF-MCS1 to create pAFSLAMcyto7. To construct pFBSLAMcyto7CAluc, the SLAMcyto7 gene was excised from pAFSLAMcyto7 and substituted for the full-length SLAM gene of pFBSLAMCAluc. All plasmids containing PCR-derived sequences were confirmed by sequence analyses. For infection with pseudotype baculoviruses bearing CD46 or SLAM, we transfected target cells with expression plasmids encoding either the hemagglutinin and fusion proteins of the Edmonston strain (EdH and EdF) or those of the Ichinose strain (IcH and IcF) measles viruses. The pCA-EdH, pCA-EdF, pCA-IcH, and pCA-IcF plasmids were kindly provided by K. Takeuchi (63).

Construction of pseudotype baculoviruses. The gp64 gene of the AcMNPV-bacmid (bMON14272; Invitrogen) was replaced with the chloramphenicol acetyltransferase (CAT) gene as described previously with slight modifications (5, 33). Briefly, the CAT gene was amplified by PCR with the Chl-Fw-*Spe*I (5′-GGACTAGTCCGAATAAATACCTGTGACGG-3′) and Chl-Rv-*Bgl*II (5′-GAAGATCTCGTCAATTATTACCTCCACGG-3′) primers using the pBT plasmid (Stratagene, La Jolla, Calif.) as a template. Following digestion with SpeI and BglII, the amplified CAT gene replaced the gp64 gene of pUCgp64locus to create p64locus/cat. To construct a gp64-null AcMNPV-bacmid, bMONΔ64/cat, the p64locus/cat plasmid was linearized by digestion with NdeI and cotransfected with bMON14272 into Sf9 cells. Forty-eight hours posttransfection, the cells were washed with cold phosphate-buffered saline and lysed in proteinase K buffer (50 mM Tris-HCl [pH 7.4], 100 mM NaCl, 1 mM EDTA, and 0.5% sodium dodecyl sulfate [SDS]). DNA was purified from cell lysates by phenol-chloroform extraction and then transformed into *Escherichia coli* DH10B competent cells (Invitrogen) by electroporation using a Gene Pulser (Bio-Rad, Hercules, Calif.). Resistant colonies were selected in kanamycin and chloramphenicol. Disruption of the gp64 gene was confirmed by PCR in a bMON14272-transformed colony that was resistant to kanamycin and chloramphenicol (Fig. 1A). To generate DH10BacΔ64/cat, we cotransfected bMONΔ64/cat and the helper plasmid pMON7124 into DH10B cells. To construct recombinant bacmids, DH10BacΔ64/cat was transformed with transfer vectors and selected according to the manufacturer's instructions. To separate recombinant bacmids from the pMON7124 helper plasmid, miniprep bacmid DNA was transformed into DH10B cells by electroporation. To generate pseudotype baculoviruses, bacmids lacking the gp64 gene and possessing both an exogenous ligand gene and the luciferase gene under the polyhedrin and CAG promoters, respectively, were transfected into Sf9 cells. Fifteen micrograms of the bacmid DNA was used to transfect 5×10^6 Sf9 cells in a 10-cm-diameter dish by using 30 μl of UniFector reagent (B-Bridge). Four days after transfection, 500 ml of culture supernatants (50 dishes) was harvested. The resulting pseudotype baculoviruses, AcΔ64/gp64/CAluc, AcΔ64/VSVG/CAluc, AcΔ64/CD46/CAluc, AcΔ64/SLAM/CAluc, and AcΔ64/SLAMcyto7/CAluc, were concentrated ~2,000 times by ultracentrifugation as described previously (66). The number of virus particles was determined from the signal intensity by Western blotting for the capsid protein vp39. Although both AcΔ64/gp64/CAluc and AcΔ64/VSVG/CAluc infected and repli-

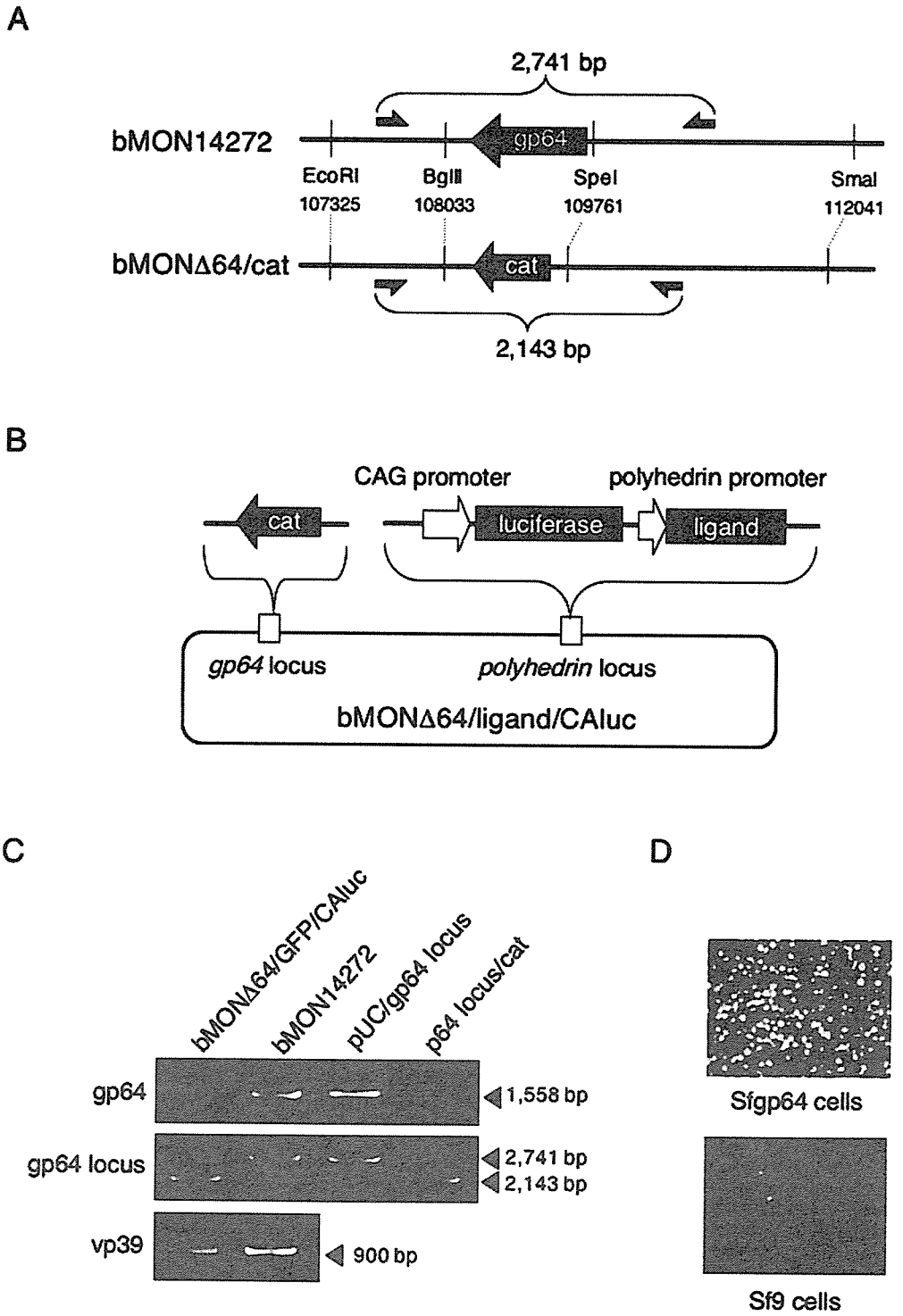

FIG. 1. (A) Schematic representations of the gp64 loci of the AcMNPV (bMON14272) and gp64-null AcMNPV (bMONΔ64/cat) bacmids. The gp64 gene (BglII/SpeI fragment corresponding to 108,033 to 109,761 nt) (3) of bMON14272 was replaced with the CAT gene by homologous recombination. The arrows indicate the locations of the PCR primers within the gp64 loci. (B) Construction of the recombinant bacmid bMONΔ64/ligand/CAluc. The gp64 gene in bMON14272 was replaced with the CAT gene. The desired ligand and luciferase genes were inserted under the control of the polyhedrin and CAG promoters, respectively, within the polyhedrin locus. (C) The bacmids bMONΔ64/ligand/CAluc and bMON14272 and plasmids containing the gp64 locus, pUC/gp64locus, and p64locus/cat (the gp64 locus with the CAT gene replacement) were amplified by PCR using primers specific for gp64, the gp64 locus, and vp39, a nucleocapsid protein of AcMNPV used as an internal control. Primers for gp64 and vp39 amplified fragments of 1,558 and 900 bp, respectively. The gp64 locus primers generated 2,741- and 2,143-bp fragments corresponding to the wild-type gp64 locus and the mutant locus with the CAT gene replacement shown in panel A, respectively. (D) Sfgp64 and Sf9 cells were transfected with bMONΔ64/GFP/CAluc. GFP expression was examined by fluorescence microscopy 4 days posttransfection.